The application of nanomaterial adsorbents for the removal of impurities from water and wastewaters: a review

Michał Bodzek[a,*], Krystyna Konieczny[b], Anna Kwiecińska-Mydlak[c]

[a]*Institute of Environmental Engineering of Polish Academy of Sciences, Marii Curie-Skłodowskiej 34, 41-819 Zabrze, Poland, email: michal.bodzek@ipis.zabrze.pl (M. Bodzek)*
[b]*Stefan Wyszynski University, Warsaw, Poland, email: k.konieczny@uksw.edu.pl (K. Konieczny)*
[c]*Institute for Chemical Processing of Coal, Zamkowa 1, 41-803 Zabrze, Poland, email: akwiecinska@ichpw.zabrze.pl (A. Kwiecińska-Mydlak)*

ABSTRACT

Nanomaterial adsorbents due to their size and high surface area to volume ratio exhibit unique properties in comparison with conventional ones and have gained significant attention from the scientific community in the last few decades. The large surface area makes nanomaterial adsorbents an effective tool for water and wastewater treatment. In this review, an attempt to the applicability of different types of nanomaterials, such as metals and metal oxides, carbon nanotubes and graphene, and various polymeric nanocomposites as adsorbents for removal of various heavy metals and organics from water environment is made. Functionalization by chemical modification often changes the character of nanoadsorbents surface and significantly improves adsorption abilities. In this paper, the metal/organics–nanomaterial interactions, mechanisms and capacities of nanomaterials based adsorption at a wide range of experimental conditions are analyzed and discussed.

Keywords: Adsorption; Nanomaterials; Review; Water and wastewater treatment

1. Introduction

Water is one of the most precious and opulent natural resources and it is essential for life on earth. Even though only less than 1% of water is directly available for humans for drinking purposes [1]. In 21st century the reliable access to clean and cheap water is a crucial global challenge. Currently, common availability of water is limited and according to Water Health Organization, almost 780 mln of people around the world still suffer from water stress [2]. This water poverty is mainly observed in developing countries, in which water and sanitary infrastructure are underdeveloped. In both, industrialized and developing countries, water scarcity mainly results from population growth, living standards improvement, climate changes as well as environmental pollution, including aquatic resources, caused mainly by anthropogenic industrial activities. In practice all-natural water reservoirs, such as surface and groundwater, lakes, rivers, channels and fall water are contaminated with various toxic substances and pathogens [3]. The main reason for the contamination is the discharge of industrial wastewater, which contains a variety of harmful chemical compounds such as dyes, toxic metals' ions, pesticides, aromatic hydrocarbons or chlorinated hydrocarbons derivatives. The increasing amount of contaminants, generated by various industry sectors, has resulted in the development of more advanced water treatment and distribution methods as well as in sharpening of water quality standards, especially in developed countries. Moreover, water pollution causes ca. 90% of all diseases notified in developing countries. There are more than 4 billion registered cases of diseases caused by the consumption of contaminated water. According to WHO almost 12 mln of people die every year because of diseases related to use and consumption of poor

* Corresponding author.

quality water [2]. Due to this fact, the municipal and industrial water and wastewater treatment plants need to apply more efficient, economically justified and environmentally friendly water and wastewater treatment methods, which allow for sustainable management of aqueous streams. Moreover, current water issues force the use of alternative water sources, such as sea or brackish water, rainwater or water reclaimed from wastewater, especially in regions of scarce water resources.

The main contaminants in water (including surface water, groundwater, and wastewater) are inorganic pollutants such as heavy metals (i.e. metals with atomic numbers greater than 20), chromium and arsenic anions, organic pollutants such as detergents, pesticides, pharmaceuticals, dyes, and others. Heavy metals usually appear in cationic form such as Pb^{2+}, Hg^{2+}, Cr^{3+}, Cd^{2+}, As^{3+}, Co^{2+}, Cu^{2+}, Ni^{2+}, Zn^{2+}, Ag^+, and others. Moreover, As and Cr may also be found as anions (i.e. arsenate AsO_4^{3-}, arsenite AsO_3^{3-}, hydrogen chromate $HCrO_4^-$, chromate CrO_4^{2-} and dichromate $Cr_2O_7^{2-}$ ions). The pollution of water caused by heavy metals and their toxic ions has become a severe environmental and public health problem because the accumulation of non-biodegradable heavy metals in the human body leads to serious diseases. Another pollution, which requires careful attention, is caused by disinfection by-products, a residue of pharmaceuticals and endocrine-disrupting compounds. Among endocrine disruptors, special attention is given to polycyclic aromatic hydrocarbons and surface-active substances, chlorinated pesticides, phthalates, alkylphenols, polychlorinated biphenyls, hormones, synthetic pharmaceuticals, and other substances disposed to the environment [4,5]. Water may be also contaminated with biologically active components, that is, viruses, bacteria, and protozoa as well as other microorganisms (fungi, algae, snails, worms and crustaceans) [6]. If such the water is to be dedicated to potable purposes, it may seriously harm human health. This hazard is also valid to treated and untreated wastewater discharged to natural water collectors and sewage systems. Among microorganisms, which appear in water, the proper removal of viruses requires the most attention due to the possibility of infection at low chlorine doses, long lifespan and poor removal efficiency during conventional water or wastewater treatment. It is commonly known, that raw municipal wastewater contains many pathogenic and opportunistic microorganisms, including ones, which are resistant to antibiotics, mainly of fecal origin. The presence of pathogenic microorganisms in wastewater is dangerous, as they may lead to epidemic effects, allergic reactions, toxic or immunotoxic health interactions to humans, animals, and other environmental species. Despite a very high reduction of bacteria in wastewater during its treatment, reaching 99%, wastewater treatment plant effluents may still contain from 10^5 to 10^7/mL of indicating fecal coliform [6]. Moreover, by-products of disinfection (DBPs) and oxidation are undesired groups of substances formed during the reaction of disinfecting agents or other strong oxidizers with admixtures and contaminants present in water. The group of DBPs mostly comprises of organic compounds, but some of inorganic substances are also included (bromates, chlorites, and chlorates) [6]. To deal with different contaminants, which appear in aqueous streams, chemical, physical and biological strategies

have been applied to remedy the problem of toxic elements, organic contaminants and bioactive materials from water and wastewater.

The conventional techniques used for the removal of inorganic and organic admixtures and impurities from water environment include chemical precipitation, adsorption, ion exchange, membrane processes, coagulation and flocculation, flotation and extraction, irradiation, electrochemical treatment techniques, advanced oxidation, and biosorption processes [4,5]. Among them, one may find techniques, which comprise a range of processes dedicated to the removal of different types of pollutants. For example, membrane processes [5] include first of all reverse osmosis, which retains monovalent ions and the majority of low-molecular compounds, next nanofiltration, which separates bivalent ions and low-molecular organic/inorganic compounds, and finally ultrafiltration and microfiltration, which are able to directly remove colloids, suspended substances and microorganisms. Nevertheless, despite the fact that conventional techniques are found to be very efficient, the majority of them require the use of either expensive chemicals or expensive devices. Hence, in most cases, two or more methods are combined to work synergistically and assure efficient remediation. The choice of the technological system for water or wastewater treatment depends on the raw stream type and properties. Groundwater may be simply purified before its distribution to the water system, while surface water and wastewater treatment are more complex due to the presence of a wider range of various types and often harmful contaminants. In addition to the classical application in drinking water treatment, other application fields are found interesting, such as groundwater remediation, treatment of landfill leachate, etc. One of the solutions to the problem of water contamination is the development of new technologies, which needs to be followed by their introduction to the practice [4].

The progress observed in the development of nanotechnology is a promising alternative for the improvement of water and wastewater treatment efficiency. Nanomaterials (NMs) (of common size range: 1–100 nm) characterize with unique physical and chemical features such as large surface area, surface activity and affinity to various chemical compounds. Hence, NMs are applied in detection and removal of heavy metals and other organic and inorganic contaminants from water. The intensive development of nanotechnology and NMs offers a significant improvement in water treatment and environmental protection methods, including the establishment of economically attractive systems for sustainable water supply. Multifunctional properties of NMs enable economically justified production of high-quality water and construction of advanced wastewater treatment systems, which, moreover, do not need to be arranged in large wastewater treatment infrastructure [3,7–11]. It is supposed that nanotechnology-based water and wastewater treatment will allow for economically balanced use of alternative water sources and will increase the possibility of production of not only potable water but also one dedicated to agriculture and industrial purposes.

Recent researches on the use of nanotechnology in water and wastewater treatment are focused on four main application areas: (a) filtration through membranes, (b) adsorptive

elimination of contaminants, (c) disinfection and (d) catalytic degradation [3,7–11]. These applications are based on nanomaterial features, that is, size, a large surface area related to fast dissolution, high reactivity, and strong sorption as well as superparamagnetism. The use of nanotechnology in wastewater treatment and water reclamation has not yet been introduced to industrial scale, however, laboratory and pilot researches have shown very promising results for the large scale implementation [6]. Additionally, even though adsorption processes have been playing a central role in water treatment for many years, their importance rises due to the identification and detection of new micropollutants in water (e.g. pharmaceuticals).

2. Adsorption

Adsorption is the unit operation commonly used to remove organic and inorganic contaminants from water and wastewater. The efficiency of conventional adsorbents is usually limited due to the small specific surface area and/or a low number of active sites, the lack of selectivity and slow rate as well as short adsorption and regeneration cycles, which significantly affects the economy of the process. Two types of interactions are distinguished in adsorption processes, that is, physical and chemical ones. Physical sorption is based on weak van der Waals forces between particles, dipole-dipole attraction and hydrogen bonding [11]. Chemisorption, that is, chemical adsorption, relies on the formation of strong chemical bonds between an adsorbent and an adsorbate. Chemisorption is single-layer adsorption, which means that on an adsorbent surface only one layer (monolayer) of an adsorbate can be adsorbed.

Nanomaterials based adsorbents, that is, nanometals and metal oxides, carbon nanotubes (CNTs), graphene and nanocomposites possess large specific surface area and corresponding, a high number of active sites suitable for sorption, high reactivity, short diffusion path inside particles, fast kinetic and specific affinity to various contaminants. Their adsorption efficiency toward some compounds is several times higher than in case of conventional adsorbents [11–14].

2.1. Carbon based nanoadsorbents

Carbon-based nanoadsorbents include CNT, graphene and nanoparticles of activated carbon. These materials characterize with large specific surface area, high thermal stability and ability to adsorb inorganic and organic contaminants [15]. Their usability to remove contaminants from water usually requires proper surface modification due to relatively poor interaction of ions (metals) and other substances with an adsorbent surface.

2.1.1. Adsorption onto activated carbon nanoparticles

Among all carbon-based nanomaterials, activated carbon nanoparticles (ACNPs) have distinct physical and chemical properties, surface morphology, uniform particle size, biocompatibility and large surface area [16]. ACNPs characterize with high heterogeneous surface functionality and appear as black crystalline to amorphous materials with meso, micro, and macro pore size. As conventional

activated carbon (AC), ACNPs can be applied in removal of toxic pollutants like heavy metals, phenols, and its derivative, which are regarded as an essential group of refractory compounds present in industrial wastewater [16–20]. AC is also well recognized and effective in removing organic chemicals from wastewater. Moreover, ACNPs have interesting antimicrobial properties [17–21]. Table 1 gives information about the classification of ACNPs based on their pore types [16].

Carbon nanoparticles can be easily synthesized from carbon-based materials like coconut shells, cooking oil, rice bran, wood, etc. by thermal combustion, chemical vapor deposition, electric arc discharge, biological methods, etc. [16]. Synthesized carbon nanoparticles are further processed by chemical, physiochemical or physical activation methods to obtain ACNPs [17]. These activation processes predominantly increase the surface area and pore size, improve thermal stability and mechanical strength creating potential applications of these materials as adsorbents [16]. The synthesis of ACNPs from bio-waste materials has recently been gaining much attention due to the increasing availability of precursor materials of eco-friendly nature and low production costs.

2.1.2. Carbon nanotubes

CNTs are one of the most important materials, which has promoted research and development in nanotechnology. There are three types of CNTs: single-walled carbon nanotubes (SWCNTs), multi-walled carbon nanotubes (MWCNT) and composite carbon nanotubes (CCNTs, including functionalized FCNTs) [22,23] (Fig. 1). Due to one dimensional structure, CNTs possess unique physical features, including mechanical, thermal and electrical ones. Parameters like diameter, length and chirality also play an important role in the characterization and functionalization of CNT.

The high adsorption efficiency of CNTs results mainly from large specific surface areas and interactions with contaminants. The CNTs surface available for adsorption is the external surface [23]. In comparison with conventional granular or powdered activated carbon, CNTs possess controlled pore size distribution and high active surface to volume ratio, which results in unique sorption efficiency. In CNTs, sorption occurs mainly due to physical interactions with non-polar compounds and chemical bonding of polar substances. The ability of sorption of CNTs mainly depends on the type of adsorbate and the type of functional groups on the adsorbent surface, such as carboxylic, hydroxyl, phenolic and amine functional groups [24,25]. The improvement of CNTs' surface with the use of functionalization methods based on oxidation, halogenation and cycloaddition methods, namely

Table 1
Pore size distribution of activated carbon

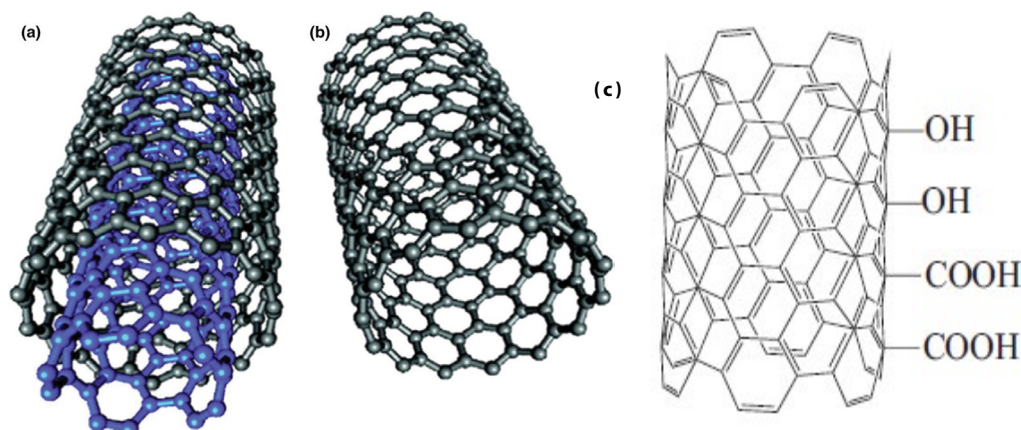| Pore type	Pore size
Micropore	<2 nm
Mesopore	2–50 nm
Macropore	>5 nm

Fig. 1. Structures of multi-walled (a), single-walled (b), and functionalized (c) carbon nanotubes [https://commons.wikimedia.org/wiki/File:Carbon_nanotube_zigzag_povray.png, https://www.cheaptubes.com/product-category/multi-walled-carbon-nanotubes/, https://en.wikipedia.org/wiki/Carbon_nanotube].

the covalent ones, has been developed. In another approach, the modification through weak interactions such as π–π and transferring charge called the non-covalent method has been proposed and both methods reportedly have their advantages. However, in some cases, modified surfaces show some disadvantages that limit the effectiveness of potential applications [26–28]. Different functional groups have been used to enhance CNTs properties, such as thiol (–SH), silane (–SiH$_4$), phenol (–OH), carboxyl (–COOH), poly(styrene-co-acrylonitrile) and amine (–NH$_2$) groups [29–33]. Also, inorganic nanoparticles have also been used in CNTs modification, for example, Fe$_3$O$_4$ and CuIn(S, Se)$_2$ [34,35]. For –NH$_2$ functionalization, various methods have been reported including ring-opening polymerization, gamma-ray irradiation, NH$_3$ plasma treatment, and the rapid microwave-assisted process [29,36–39]. On the other hand, the sorption ability is also observed for non-functionalized CNTs. The sorption effect of CNTs is the highest at pH range from 7 to 10, while outside this pH range, ionic substances disturb the sorption ability of CNTs [11,12].

In aqueous phase, CNTs form loose aggregates due to hydrophobicity of their surface, which decreases their specific surface. On the other hand, CNTs' aggregates contain spaces and interlayer channels, which reveal high adsorption ability toward organic compounds [40]. Despite the fact that conventional activated carbon characterizes with the specific surface comparable to the CNTs' one, it contains a number of micropores, which are unavailable for large organic compounds such as antibiotics and other pharmaceuticals [41]. Thus, CNTs reveal much higher sorption capacity to a certain group of large molecular weight organic compounds due to larger pores and more available sorption sites.

The strong sorption of many polar organic compounds results from various interactions of CNTs with contaminants, including hydrophobic effect, π–π interactions, hydrogen, and covalent bonding and electrostatic interactions [24]. CNTs' surface is –π–electrons rich, which allows for π–π bonds formation with organic compounds containing C=C bonds or benzene rings, such as in case of polyaromatic hydrocarbons (PAHs) and polar aromatic compounds [42].

Organic compounds, which possess functional groups like –COOH, –OH, –NH$_2$ may form hydrogen bonds with graphite CNTs surface, which becomes an electron donor [43]. The electrostatic attraction enables adsorption of organic compounds, which at suitable pH are positively charged, for example, some antibiotics [41].

CNTs have been investigated in regard to the removal of dyes from water and wastewater. Organic dyes are highly toxic already at very low concentrations in water due to their potential carcinogenic effect. For example, researches, in which multi-walled CNTs impregnated with chitosan hydrogel have been used to remove Congo red from aqueous solutions [44], have been carried out. The impregnation with chitosan hydrogel has increased porosity and thickness of the modified adsorbent. The maximum adsorption of Congo red (423.1 mg/g) has been obtained at pH 4.0. Adsorption results have shown that the Langmuir model better correlates with experimental data, while kinetics' research has revealed that the adsorption can be described with pseudo-second-order equation. SWCNTs have also been used to remove reactive Red 120 dye from textile wastewater in dependence on pH. The optimal parameter value has been established at 5.0, while below or above it the adsorption efficiency has been lower. At initial dye concentration 50 mg/L and pH = 5.0, SWCNTs possess adsorption capacity equal to 426.5 mg/g and removal efficiency reaching 85.3%. It has been found that the dye adsorption efficiency increases with the adsorbent dose increase and reaches 882.84 mg/g at equilibrium contact time 180 min [45]. The adsorption capacity of Procion MX-5B red dye during the treatment of different types of industrial wastewater with multi-walled CNTs has been investigated by Wu et al. [46]. The obtained results have shown that adsorption efficiency increases with temperature increase as mobility of dye particles increases, which confirms, that adsorption process is endothermic. At pH 6.5, the maximum adsorption equal to 20.93, 22.87, 27.20 and 30.53 mg/g has been reached during 3 h process carried out at temperatures 281, 291, 301 and 321 K, respectively. It has also been found, that Langmuir isotherm and pseudo-second-order kinetic model are suitable to describe this dye adsorption.

Promising results have been obtained in removal of natural organic matter (NOM) from aqueous solutions using multi-walled CNTs due to their hydrophobicity [47]. NOM undergoes ionization in surface and groundwater at pH range 3.0–9.0 and strong adsorption (2.5–50 mg C/L) on CNTs' surface is observed. The research has shown that Langmuir and Freundlich isotherms correspond to experimental results.

The adsorption of trihalomethanes, that is, chloroform, dichlorobromomethane, dibromochloromethane, and bromoform has also been investigated in different water types using multi-walled CNTs [48]. It has been found that chloroform adsorption equilibrium is reached faster than ones of dichlorobromomethane, dibromochloromethane, and bromoform due to smaller particle size and easier permeation of pores interior. Additionally, it has been shown that the increase of temperature from 5°C to 35°C decreases the adsorption efficiency. At 5°C maximum adsorption capacity of chloroform, dichlorobromomethane, dibromochloromethane, and bromoform has reached 3,158; 2,016; 2,008 and 1,976 mg/g, respectively.

Functionalized CNTs reveal high adsorption capacity toward metal ions. Surface functional groups of CNTs (carboxylic, hydroxyl and phenolic ones) are main adsorption sites for metal ions, mainly due to electrostatic attraction and chemical bonding [49]. Resulting surface oxidation may significantly increase the adsorption ability of CNTs. A number of researches show that CNTs are much better adsorbent than activated carbons in regard to heavy metals (Cu^{2+}, Pb^{2+}, Cd^{2+}, and Zn^{2+}) [11,34,49–55] (Table 2), and kinetics is higher for CNTs due to easily accessible adsorption sites and short diffusion path to particle interior.

Gupta et al. [55] have investigated the removal of chromium(III) using multi-walled CNTs, including ones containing ferric oxide nanoparticles, functionalized with carbonyl and hydroxyl group. The available, additional active sites formed by oxygen atoms from iron (III) oxide nanoparticles have been involved in chromium (III) adsorption. The nanocomposite has been found efficient in removal of chromium (III) at pH range of 3.0–7.0 due to formation of $Cr(OH)^{2+}$ ions.

Regeneration potential is a very important feature, which determines the usability of any adsorbent. The adsorption of metal ions on CNTs is a reversible process enabled by solution's pH decrease. The recovery rate of a metal is usually above 90%, while at pH < 2 it often reaches 100% [56]. Additionally, the sorption capacity is stable, even after regeneration. For example, adsorption capacity of Zn^{2+} ions indicated by SWCNTs and MWCNTs has decreased by 25% after 10 regeneration cycles and reuse of adsorbents, while in the case of conventional activated carbon species, it has decreased by 50% already after first regeneration cycle [57]. Statistical analysis based on Zn^{2+} adsorption capacity regression and number of regeneration and reuse cycle suggests, that CNT nanoadsorbents can be regenerated and reused up to several hundred times in case of Zn^{2+} removal at reasonable adsorption capacity maintenance [57].

The discussed examples indicate that CNTs can be potential adsorbents for removal of dyes, toxic metals, organic matter and trihalomethanes from aqueous solutions, which makes them applicable to industrial wastewater treatment. However, their practical use is currently limited due to economic reasons. Moreover, the toxicity of functionalized CNTs is not sufficiently described in the literature.

2.1.3. Adsorption onto graphene

Graphene is a layer of tightly packed carbon atoms, which are bonded together in a honeycomb shape matrix (Fig. 2a), while as it is of a single atom thickness of ca. 0.3 nm, its spatial structure is simplified to 2D [58,59]. It is an allotrope of carbon, built of planar atoms bonded with strong sigma bonds of sp^2 hybridization and of very short length (0.142 nm) [58]. Graphene characterizes with a large specific surface, unique flexibility, relatively high conductivity (above 10^2 S/m) [59] and significant mechanical strength (100–300 higher than steel, tensile strength – 130 GPa and Young modulus – 1 TPa) [60], and it is also a great mobile charge carrier [61].

Graphene surface may be simply modified, as sp^2 hybridization of carbon in graphene may reveal various interactions with polymeric matrices such as electrostatic, covalent, noncovalent (e.g. π–π interactions) interactions and it easily mixes with polymers [11]. Graphene oxide (GO) is a single-layer oxidized graphene with oxygen-containing functional groups, mainly hydroxyl, carboxyl, carbonyl and epoxy ones (Fig. 2b) [59]. Reduced graphene oxide (RGO) possesses more defects and smaller conductivity than graphene, but its modification with various functional groups is easier [59]. Thus, it characterizes with excellent hydrophilicity and better reactivity with a number of contaminants [62].

The characteristic feature of GO, due to the presence of oxygen atoms in functional groups, are easy electrostatic interactions with organic and inorganic contaminants. The adsorption on graphene-based nanomaterials may also run due to hydrophobic interactions and π–π, hydrogen or covalent bonds formation [11]. A number of papers dedicated to graphene oxide-based adsorbents and their use to removal of inorganic contaminants from aqueous solutions [62], especially metal ions from wastewater [63], have been published.

Graphene and its modified forms (GO/RGO) have been widely used to remove such heavy metals like Pb(II), Zn(II), Cu(II), Cd(II), Hg(II) and As(III/V). Wang et al. [64] have investigated the impact of pH, GO dose, presence of other ions and contact time on the efficiency of Zn(II) adsorption. The results have shown that optimum pH for Zn(II) removal equals 7.0 at relatively fast reached equilibrium. The maximum adsorption capacity of Zn(II) has reached 246 mg/g.

Madadrang et al. [65] have been found, that GO modification with EDTA allows for efficient adsorption of Pb(II) due to its chelating properties. It has been shown, that adsorption capacity can obtain ca. 480 mg/g at pH 6.8, while the equilibrium is reached within 20 min. Huang et al. [66] have also discussed Pb(II) adsorption using oxidized and pure graphene sheets. In the design of composite adsorption materials, graphene and graphene oxides nanosheets can be combined with metal oxides to form adsorbents suitable to remove various contaminants from wastewater. Kumar et al. [67] have used magnetic nanocomposite of GO with Fe(II) manganite to efficiently remove Pb(II) and As(III/V) from contaminated water. The maximum sorption capacity has been established at 673 mg/g for Pb(II), 146 mg/g for As(III) and 207 mg/g for As(V). The advantage of the

Table 2
Adsorption of heavy metal ions at different types of carbon nanotubes (CNT)

| Metal ion	Nanoadsorbent	Adsorption efficiency and process conditions	Reference
Pb(II)	CNTs (HNO_3)	49.95 mg/g at pH = 7.0; and room temperature	[50]
	CNTs	11.2 mg/g at pH = 5.1; C_0 = 10 mg/L; and room temperature	[51]
	CNTs	1.41 mmol/g	[52]
	CNTs-OH	2.07 mmol/g	[52]
	CNTs-$CONH_2$	1.907 mmol/g	[52]
	CNTs-COO^-	4 mmol/g	[52]
	MWCNTs (HNO_3)	49.95 mg/g at pH = 7.0; C_0 = 2–14 mg/L; and room temperature	[49]
Cd(II)	CNTs (HNO_3)	10.86 mg/g at pH = 7.0; and room temperature	[50]
	CNTs-COO^-	3.325 mmol/g	[52]
	CNTs-OH	1.513 mmol/g	[52]
	CNTs-$CONH_2$	1.563 mmol/g	[52]
	CNTs	1.29 mmol/g	[52]
	CNTs	1.1 mg/g at pH = 5.5; C_0 = 9.5 mg/L; and T = 25°C	[49]
	CNTs (H_2O_2)	2.6 mg/g at pH = 5.5; C_0 = 9.5 mg/L; and T = 25°C	[49]
	CNTs ($KMnO_4$)	11.0 mg/g at pH = 5.5; C_0 = 9.5 mg/L; and T = 25°C	[49]
	CNTs (HNO_3)	5.1 mg/g at pH = 5.5; C_0 = 9.5 mg/L; and T = 25°C	[49]
Ni(II)	MWCNTs	7.53 mg/g at pH = 7.0	[52]
	SWCNTs	9.22 mg/g at pH = 7.0	[53]
	MWCNTs (HNO_3)	9.80 mg/g at pH = 6.55; C_0 = 6–20 mg/L; and T = 60°C	[49]
	SWCNTs	9.22 mg/g at pH = 7.0 and T = 25°C	[49]
	SWCNTs (NaOCl)	47.85 mg/g at pH = 7.0 and T = 25°C	[49]
	MWCNTs	7.53 mg/g at pH = 7.0 and T = 25°C	[49]
	MWCNTs (NaOCl)	38.5 mg/g at pH = 7.0 and T = 25°C	[49]
	MWCNTs (HNO_3)	17.86 mg/g at pH = 6.5; C_0 = 10–30 mg/L; and T = 25°C	[11]
Zn(II)	SWCNTs	11.23 mg/g at pH = 7.0; C_0 = 10–80 mg/L; and T = 25°C	[49]
	SWCNTs (NaOCl)	43.66 mg/g at pH = 7.0; C_0 = 10–80 mg/L; and T = 25°C	[49,54]
	MWCNTs	10.21 mg/g at pH = 7.0; C_0 = 10–80 mg/L; and T = 25°C	[49]
	MWCNTs (NaOCl)	32.68 mg/g at pH = 7.0; C_0 = 10–80 mg/L; and T = 25°C	[49,54]
Cu(II)	CNTs (HNO_3)	10.86 mg/g at pH = 7.0 and room temperature	[50]
	CNTs	1.219 mmol/g	[52]
	CNTs-OH	1.342 mmol/g	[52]
	CNTs-$CONH_2$	1.755 mmol/g	[52]
	CNTs-COO^-	3.565 mmol/g	[52]
Hg(II)	CNTs/MnO_2	58.8 mg/g at pH = 6.05; C_0 = 1–50 mg/L; and T = 25°C	[11]
	CNTs/Fe_2O_3	238.78 mg/g pH = 4; C_0 = 10–50 mg/L; and T = 25°C	[34]
Cr(VI)	CNTs/nZVI	3.1–3.3 mg/g at pH = 7.0; C_0 = 1–10 mg/L; and T = 25°C	[11]
	CNTs/Fe_2O_3	90% removal at pH = 3–7; C_0 = 20 mg/L; and T = 25°C	[55]
Se	CNTs/nZVI	1.1–3.7 mg/g at pH = 7.0; C_0 = 1–10 mg/L; and T = 25°C	[11]
Co	CNTs/nZVI	1.7–4.8 mg/g at pH = 7.0; C_0 = 1–10 mg/L; and T = 25°C	[11]
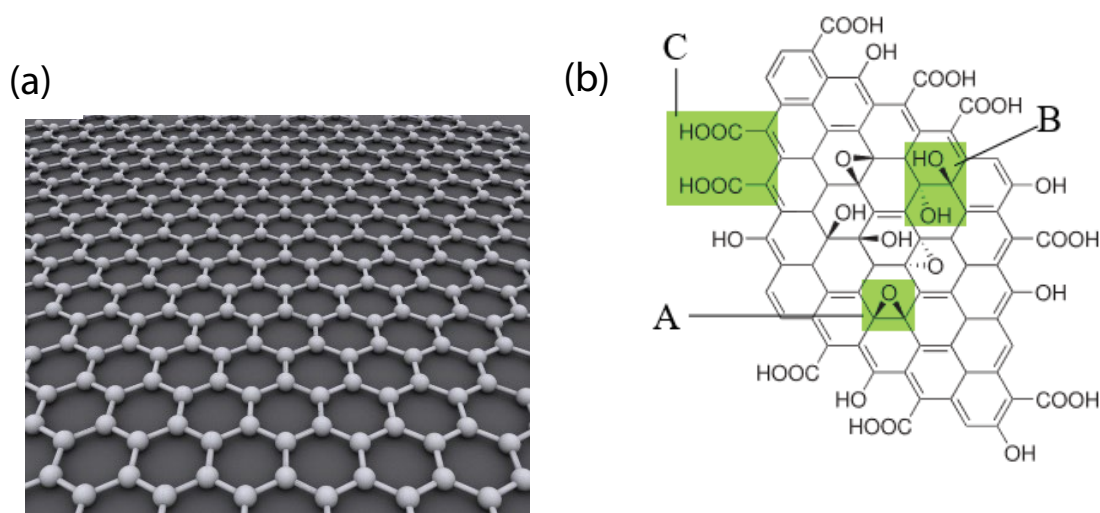
Fig. 2. (a) Two-dimensional model of graphene structure and (b) graphene oxide (GO) model [https://en.wikipedia.org/wiki/Graphene, https://en.wikipedia.org/wiki/Graphite_oxide].

adsorbent, except for its high capacity, is its simple separation in magnetic field. Another example is the removal of toxic metals ions like lead(II), zinc(II) and cadmium(II) from aquatic environment by means of adsorption with composite material composed of graphene oxide/titanium dioxide [68]. The efficiencies of adsorption of lead(II), zinc(II) and cadmium(II) have reached 65.6, 88.9, and 72.8 mg/g, respectively, at pH 5.6. The adsorption capacity of the composite material has been higher than one of graphene oxide or titanium dioxide themselves. The results of the removal efficiency of various metals using GO-based adsorbents are presented in Table 3.

Except for metal ions removal, graphene-based adsorbents have also been investigated in regard to adsorption of anionic contaminants. Li et al. [76] have stated, that graphene is a good adsorbent for fluorides and possess adsorption capacity equal to 36.5 mg/g at pH 7.02 and 25°C. The mechanism of adsorption relies on the exchange of fluorides present in solution to hydroxyl ions present in adsorbent structure. Vasudevan and Lakshmi [77] have performed systematic research on phosphates adsorption on graphene. The experimental results have shown that graphene adsorption capacity reaches 89.37 mg/g. Zhang et al. [78] have developed a hybrid composite of graphene-polypyrrole (Ppy) to remove perchlorates (ClO_4^-). The composite has characterized by higher perchlorates sorption capacity than single Ppy films, while the adsorption mechanism has relied on ion exchange.

Hartono et al. [79] have investigated humic acids (HA) adsorption using GO. The maximum adsorption capacity has reached 190 mg/g, which is, much higher than the one of activated carbon. The adsorption of antibiotics like tetracycline, oxytetracycline, and doxycycline [80] and dyes [81,82] on GO has also been checked. It has also been found that the mechanism of ionic dyes adsorption relies mainly on electrostatic interactions and covalent bonding. Due to this fact, GO reveals high adsorption efficiency in regard to cationic dyes, while its affinity to anionic dyes is limited due to strong electrostatic repulsions. On the other hand, graphene and graphene composites may be good adsorbents for anionic dyes if ion exchange or covalent bonding are involved in adsorption mechanism [81]. The results of the research on antibiotics and dyes removal from wastewater using grapheme-based adsorbents are shown in Table 4.

In many cases, modification and hybridization of a sorbent surface area are effective methods of improvement of adsorbents usability and they increase the efficiency of contaminants removal on grapheme-based materials. However, their high costs limit the common application. There are also some other issues, which need to be solved, including multiple reuse, environmental safety and compatibility with other processes.

2.2. Metal/metal oxide based nanomaterials

Due to the unique sorption properties of metal and metal oxides nanoparticles (NPM, NPMO) they are widely used to remove contaminants from wastewater [11]. The most popular NPMs and NPMOs are zero-valent iron [12,13], silver [99] and gold [100] as well as magnetic iron oxides [101], manganese oxides [102], titanium oxide [103], magnesium oxide [104], copper oxide [105], cerium oxide [106], aluminum oxide, etc. [107]. Many researches confirm that metals nanoparticles (NPM) and NPMO reveal highly efficient and selective sorption of contaminants like arsenic [108], cadmium [109], chromium [110] and other metal ions [109] as well as typical anionic contaminants, for example, phosphates [111] and organic contaminants [112]. Due to large specific surface, these nanosorbents possess short internal diffusion pathways and do not undergo significant compression, which would lead to the surface decrease. Table 5 summarizes the most important properties, applications, and innovative approaches involving nano-metals and nanometal oxides [113]. Still, the applicability of nanometals and nanometal oxides in water and wastewater treatment sector strongly depends on the efficiency (nano-TiO_2) and stability of the metals (magnetic nanoparticles, nano-zero-valent iron, nano-silver).

Table 3
Graphene nanocomposites used in removal of metal ions

Metal	Graphene nanocomposite	Adsorption efficiency (mg/g)	Reference
		Experiment conditions	
Cu(II)	GO	75 at pH = 5.0; T = 30°C	[69]
	Graphene oxide (GO)/Fe$_3$O$_4$	18.3 at pH = 5.3; T = 20°C	[70]
	GO/Fe$_3$O$_4$/sulfanilic acid	50.7–56.8 at pH = 3–5	[71]
	Graphene/MWCNT	33.8 at room temperature	[69]
	GO/Mn-doped Fe(III)oxide	130–144 at pH = 5.1; T = 25°C–30°C	[72]
	PVP-RGO	1,689 at pH = 3.103	[8]
	GO/CdS	1,347.2 at pH = 6.0; T = 25°C	[69]
	Graphene/d-MnO$_2$	103 at pH = 6.0; T = 25°C	[69]
Pb(II)	Graphene nanosheet	4,605 at pH = 5.5; T = 20°C	[69]
	GO	328 at pH = 6.1; T = 25°C	[69]
	GO/Fe$_3$O$_4$	38.5 at pH = 5.5; T = 20°C	[71]
	GO/silica/Fe$_3$O$_4$	333.3 at pH = 7.8; T = 25°C	[73]
	GO-MnFe$_2$O$_4$	673 at pH = 5.0; T = 25°C	[67]
	GO/CoFe$_2$O$_4$	299.4 at pH = 5.3; T = 25°C	[71]
	TiO$_2$/GO	65.6 at pH = 5.6; T = 25°C	[68]
	GO-EDTA	479 at pH = 6.8 and room temperature	[65]
	SiO$_2$-Graphene	113.6 at pH = 6.0; T = 25°C	[74]
Cd(II)	GO/silica/Fe$_3$O$_4$	166.7 at pH = 6.1; T = 25°C	[73]
	GO/Mn-doped Fe(III)oxide	88–127 at pH = 5.1; T = 25°C–30°C	[72]
	TiO$_2$/GO	72.8 at pH = 5.6; T = 25°C	[68]
	GO/Fe$_3$O$_4$	4.4 at pH = 5.5; T = 20°C	[71]
Zn(II)	GO	246 at pH = 6.0	[64]
	TiO$_2$/GO	88.9 at pH = 5.6; T = 25°C	[68]
Hg(II)	GO	35.25 at pH = 6.0 and room temperature	[69]
	Graphene/MWCNT	75.6 at room temperature	[69]
	CoFe$_2$O$_4$/RGO	158 at pH = 4.6; T = 25°C	[69]
	Polypyrrole/RGO	979.5 at pH = 3.5; T = 20°C	[69]
As(III)	GO-ZrO	60–81 at pH = 7.0; C_0 = 2–80 mg/L; and T = 25°C	[11]
	Fe$_3$O$_4$/SiO$_2$/GO	7.51 at pH = 4; T = 25°C	[69]
	GO-MnFe$_2$O$_4$	146 at pH = 6.5; T = 25°C	[69]
	GO/Fe$_3$O$_4$/TiO$_2$	77.7 at pH = 6–7; T = 30°C	[69]
As(V)	GO-ZrO	55–83 at pH = 7.0; C_0 = 2–80 mg/L; and T = 25°C	[11]
	Fe$_3$O$_4$/SiO$_2$/GO	11.5 at pH = 4; T = 25°C	[69]
	GO-MnFe$_2$O$_4$	207 at pH = 4; T = 25°C	[69]
	GO/Fe$_3$O$_4$/TiO$_2$	99.5 at pH = 6–7; T = 30°C	[69]
Cr(III)	GO	27.16 at room temperature	[69]
	GO	92.65 at pH = 5; T = 23°C	[69]
	Poly(amidoamine)/GO	55.82 at room temperature	[69
Cr(VI)	GO	65.23 at pH = 7	[69]
	Nano-Fe/graphene	162.6 at pH = 4.25; T = 20°C	[69]
	Fe$_3$O$_4$/GO	32.33 at pH = 4.5; T = 23°C	[69,11]
	GOGO/Fe$_3$O$_4$/polypyrrole	348 at pH = 2.0; T = 25°C	[8]
	PEI-GO	539.5 at pH = 3.5; T = 35°C	
Ni(II)	Graphene/d-MnO$_2$	46.5–66 at pH = 7.0; C_0 = 1–100 mg/L; and T = 25°C	[11]
Fe(III)	GO aerogel	133.33	[75]

Table 4
Adsorption of organic contaminants using graphene based materials

Contaminant	Graphene-based nanocomposite	Sorption capacity (mg/g)	Reference
Methylene blue	Polyethersulphone/GO	62.50 at pH = 7 and T = 30°C	[83]
	Fe_3O_4/GO	167.2	[84]
	Sponge	397 at pH = 7 and T = 25°C	[81]
	RGO/CdS	94% at 5% RGO in solution	[15,85]
	RGO-$MnFe_2O_4$	100% at C_0 = 5 mg/L, 0.6 g/L RGO and T = 20°C	[86]
	GO	351	[87]
	GNs	154–204 at C_0 = 5 mg/L, 0.6 g/L RGO and T = 20°C	[86]
	CNTs	35.4 at pH = 7 and T = 0°C	[88]
	CNTs	46.2 at pH = 7 and T = 25°C	[88]
	CNTs	64.7 at pH = 7 and T = 60°C	[88]
	Graphene-CNTs	65.8 at pH = 7 and T = 10°C	[88]
Rhodamine B	RGO-$MnFe_2O_4$	87.2 at pH = 7; C_0 = 60 mg/L; and T = 25°C	[89]
Methylene violet	GO sponge	467 at pH = 7 and T = 25°C	[81]
Malachite green	MWCNTs	142.85 at pH = 7 and T = 25°C	[88]
	MWCNTs	55.25 at pH = 8 and T = 25°C	[88]
	MWCNTs	41.15 at pH = 8 and T = 45°C	[88]
	MWCNTs-COOH	11.63 at pH = 98 and T = 55°C	[88]
	MWCNTs-SH	166.7 at pH = 6 and T = 25°C	[88]
	SWCNTs	4.9825 at pH = 7 and T = 27°C	[88]
	SWCNTs-NH_2	6.134 at pH = 7 and T = 27°C	[88]
	SWCNTs-COOH	19.84 at pH = 7 and T = 27°C	[88]
Basic red	SWCNTs	38.35 at pH = 9 and T = 25°C	[88]
	SWCNTs-COOH	49.45 at pH = 9 and T = 25°C	[88]
Congo red	MWCNTs	148 at pH = 7 and T = 25°C	[88]
	MWCNTs	232 at pH = 11 and T = 25°C	[88]
	CNTs/Mg(Al)O	1,250 at pH = 6.5 and T = 25°C	[88]
	MWCNTs/ZnO	249.5 at T = 55°C	[90]
Reactive blue 4	MWCNTs	502.5 at pH = 2 and T = 25°C	[88]
	SWCNTs	568 at pH = 2 and T = 25°C	[88]
BisphenolA	GO/β-cyclodextrin	373.4 at pH = 9; C_0 = 100 mg/L; and T = 25°C	[91]
Ciprofloxacin	Graphene hydrogel	235.6 at pH = 6–8; C_0 = 100 mg/L; and T = 25°C	[92]
	KOH-graphene	194.6	[93]
	Single layer GO	379 at pH = 5 and T = 25°C	[94]
Tetracycline	TiO_2-graphene sponge	1,805	[95]
	GO	323 at pH = 6–7 and T = 25°C	[96]
	F-GO and MNPs	39.1 at pH = 8–9; C_0 = 0–100 mg/L and room temperature	[97]
	GO	313.48 at pH = 3.6 and T = 25°C	[80]
	SWCNTs	340	[80]
	MWCNTs	100	[80]
Doxycycline	F-GO and MNPs	35.5 at pH = 8–9; C_0 = 0–100 mg/L and room temperature	[97]
	GO	398.40 at pH = 3.6 and T = 25°C	[80]
Oxytetracycline	GO	212.31 at pH = 3.6 and T = 25°C	[80]
	F-GO and MNPs	45.0 at pH = 8–9; C_0 = 0–100 mg/L; and room temperature	[97]
Chlortetracycline	F-GO and MNPs	42.6 at pH = 8–9; C_0 = 0–100 mg/L; and room temperature	[97]
Microorganism *E. coli*	MWCNTs-Ag	99.98% inactivation at pH = 9 and T = 25°C	[98]
	MWCNTs-ZnO	100% inactivation at room temperature	[98]
	SWCNTs-Ag-Fe_3O_4	100% inactivation at 25°C	[98]
Bacillus megaterium	SWCNTs-Ag-Fe_3O_4	100% inactivation at 25°C	[98]
Microorganism *Proteobacteria*	MWCNTs	62.5% inactivation at pH = 7.2–7.6 and 21°C	[98]

Table 5
Properties, applications, and innovative approaches for nanometals and nanometal oxide

| Nano-metals and nano-metal oxides | Properties | | Applications | Novel approaches |
	Positive	Negative		
Nano-silver and nano-TiO$_2$	Bactericidal, low human toxicity Nano-TiO$_2$: high chemical stability, very long life time	Nano-silver, limited durability, Nano-TiO$_2$, requires ultraviolet activation	Point-of-use water disinfection, antibiofouling surfaces, decontamination of organic compounds, remote areas	TiO$_2$ modification for activation by visible light TiO$_2$ nanotubes
Magnetic nanoparticles	Simple recovery by magnetic field	Stabilization is required	Groundwater remediation	Forward osmosis
Nano zero-valent iron	Highly reactive	Stabilization is required (surface modification)	Groundwater remediation (chlorinated hydrocarbon, perchlorates)	Entrapment in polymeric matrices for stabilization

Some NPMOs (e.g. nanomaghemite or nanomagnetite) possess paramagnetic properties, what favors their separation and recovery in low-gradient magnetic field [113]. Magnetic NPMOs are composed of a magnetic core and a coating/shell [113] and a core can be made of cobalt, iron, nickel and their oxides or alloys of ferromagnetic or superparamagnetic properties, whereas coatings can be formed from inorganic components like silica [114] and aluminum oxide [115] or from organic components like polymers [116] or surface active agents (Fig. 3). In regard to stability and recycling of NPMs and NPMOs coats play a very important role [117], especially in the case of small organic particles, organic polymers (polystyrene, polyaniline or biopolymers like cellulose or chitosan) or inorganic supports. Additionally, NPMs can be used as adsorptive filters and in suspended bed reactors [6,118].

2.2.1. Nanometals

Recently, information on the use of various metals nanoparticles, mainly iron, silver, gold, nickel, aluminum and zinc, in wastewater treatment [6] can be found in literature. In Table 6, standard reduction potentials of different metals are presented [6].

2.2.1.1. Zero-valent iron

Zero-valent iron (ZVI) is efficient material to water treatment, especially when it appears as zero-valent nano-iron (nZVI). nZVI characterizes with high reactivity with a wide range of contaminants due to large specific surface and number of active sites as well as small particle size [119] in comparison with regular ZVI. Some researches have shown, that by the decrease of size of ZVI from microscale to nanoscale, the rate of removal of As(V) can be three times increased [107]. Additionally, nZVI surface can be easily modified, reveals excellent magnetic properties and high biocompatibility [120]. nZVI nanoparticles possess core-coat structure with an external layer of iron oxides and internal Fe^0 core (Fig. 3). Iron oxide layer around Fe^0 core has been recognized as a strong adsorbent. Fe^0 core can be oxidized
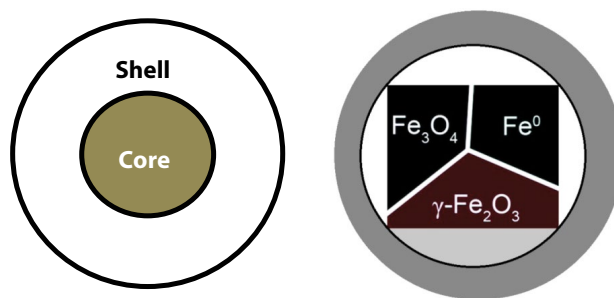

Fig. 3. Exemplary scheme of a magnetic nanoparticle composed of a magnetic core and a coat.

Table 6
Standard reduction potentials of different metals

Metal	Standard reduction potential (E/V)
Nickel	–0.236
Zinc	–0.762
Iron	–0.440
Aluminium	–1.677

to iron oxides in reaction with water, and next it can be transformed to a number of corrosion products, including goethite (α-FeOOH), akaganeite (β-FeOOH), lepidocrocite (γ-FeOOH), magnetite (Fe$_3$O$_4$), maghemite (γ-Fe$_2$O$_3$) or green siderite (FeCO$_3$). These corrosion products also reveal significant adsorption affinity to large amounts of contaminants [121]. Fig. 4 shows the mechanisms of removal of metal ions and some organics from the water environment.

nZVI are widely used as adsorbents in contaminants removal from water/wastewater. Hua et al. [107] have shown complete removal of As(V) using nZVI adsorbent doses equal to 0.1, 0.2 and 0.4 g/L introduced to three different types of real wastewater. The research has also shown that As(V) adsorption occurs due to complexation at the internal nZVI layer [107]. It has also been found that many metals like
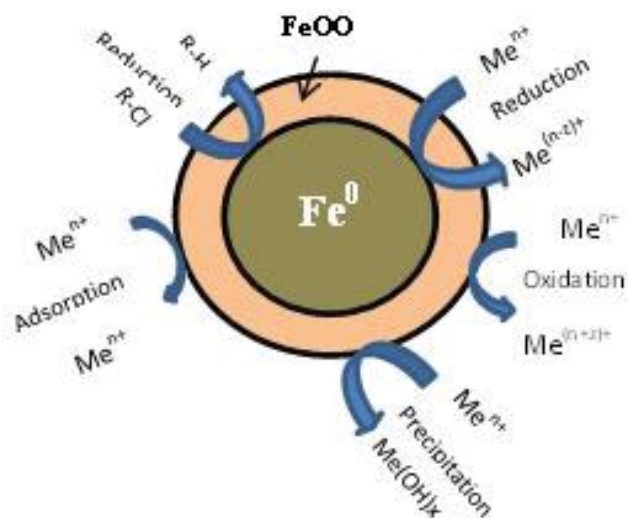
Fig. 4. Core-shell structure of nZVI depicting various mechanisms for the removal of metals and chlorinated compounds.

cadmium [109], chromium [110], etc. are also adsorbed by nZVI due to formation of complexes with internal components of nZVI.

Some contaminants like As(III/V), U(VI), Se(VI) can decrease their oxidation state by adsorption on nZVI surface. Crane et al. [122] have stated, that U(VI) can be removed by nZVI adsorption to a concentration below 10 µg/L (>98% removal) within 2 h, and it can be partially reduced to U(IV) at simultaneous oxidation of Fe. Li et al. [123] have shown, that the average adsorption capacity of Cu(II) on nZVI equals 343 mg/g due to reduction to metallic copper or cuprite (Cu_2O). Ramos et al. [124] have found, that As(V) or As(III) is partially reduced to As(0) after reaction with nZVI. Additionally, As(III) forms As(0), As(III) and As(V) on nZVI surface, what means that during the reaction both, reduction and oxidation of As(III) occurs. Double redox function of nZVI is possible due to core-coat structure, as the core is the metallic iron of strong reduction tendency, while the external layer containing thin, amorphous iron oxides/hydroxides promotes coordination and oxidation. Despite above-mentioned ions, nZVI can also remove phosphates [111], nitrates [125], dyes [112] and antibiotics [126] due to physical adsorption, oxidation, reduction, and co-precipitation mechanisms.

To sum up, nZVI is highly reactive, economically attractive and environmentally friendly adsorption material which can be used in water and wastewater treatment.

2.2.1.2. Gold nanoparticles

Nanoparticles of gold have been used to remove heavy metals' ions from water, mainly with the coat containing 4-aminothiophenol [127]. For removal of Hg^{2+} or Pb^{2+} ions from aquatic solutions, a composite of nanogold and albumin bovine (BSA) coated with gel agarose membrane (Au NPs@ BSA/AGM) have been developed [128], and additionally, to Hg^{2+} ions adsorption, gold nanoparticles functionalized with magnetic silica sphere (MSS) [127] have been made.

2.2.1.3. Silver nanoparticles

Nanosilver has been used in photodegradation processes since the end of 1800, while in 1954 it was registered by EPA as the biocide for pools and in 1970 for potable water filters [129]. Moreover, nanosilver reveals strong and wide antibacterial activity, while it is harmless to humans. It is also used in point-of-use disinfection and anti-biofouling surfaces materials [129].

Such the effect is obtained due to the release of Ag^+ ions and generation of products containing reactive oxygen species [130]. Antibacterial action of silver nanoparticles can be controlled and in opposite to silver ions it is permanent. The reaction of silver salt with a reducer on an adsorbent surface results in uniform and irreversible coating of the surface with Ag nanoparticles. The layer of nanoparticles formed at the surface results in strong antibacterial properties.

It has been found that silver nanoparticles (NPs) are highly toxic to microorganisms, thus they can destruct fungi [130], bacteria [131] and viruses [132]. Due to this feature, Ag NPs are widely used in water disinfection. Ag NPs sheets reveal efficient antibacterial effects to *Enterococcus faecalis*, *Escherichia coli*, and deactivate bacteria cells during filtration. It has been found that Ag NPs interact with a bacteria cell's walls, next reach the cell interior and deform the cell's wall structure increasing its permeability [133]. During Ag NPs interaction with a cell, free radicals can also be formed, thus the cell wall is damaged and the microorganism dies [133]. Several theories on antibacterial Ag NPs action are available, whereas the deactivation mechanism has not been yet completely recognized and it is still discussed.

Ag NPs have been efficiently applied to wastewater treatment. The main disadvantage of this material is the formation of clusters in water by non-modified Ag NPs, which affects its antibacterial properties during long-term use [76]. On the other hand, systems integrating Ag NPs with membranes or filters are used to water disinfection due to the efficient antibacterial effect and low costs [134].

2.2.1.4. Zinc nanoparticles

Zinc nanoparticles are found to be an alternative solution for Ag and Fe NPs [135]. With their highly negative standard reduction potential (Table 4), Zn NPs are much stronger reducing agents than Fe NPs. Hence, the ability of contaminants degradation by Zn NPs is faster and more efficient. The use of Zn NPs is related to wastewater dechlorination, degradation of carbon tetrachloride and octachlorodibenzo-p-dioxin [136]. The degradation of the latter in wastewater has been investigated using nanoparticles of four different metals, that is, nickel, aluminum, iron, and zinc. At optimum reaction conditions, the highest efficiency of octachlorodibenzo-p-dioxin degradation has been reached with the use of zinc nanoparticles. Hence, Zn NPs are the first nanomaterial registered to degradation of octachlorodibenzo-p-dioxin [135]. It has been found that the effectiveness of the process depends more on the physico-chemical properties of contaminants than on their size or surface morphology. There are, however, not too many researches dedicated to the removal of other contaminants from water or wastewater using Zn NPs [136].

2.2.2. Metal oxides nanoparticles

Metal oxides, mainly iron oxide, titanium dioxide, aluminum oxide and other, are efficient and cheap adsorbents for heavy metals and radionuclides removal from aqueous streams. Sorption is mainly controlled by complexation of dissolved metal ions with oxygen from metal oxides, and it is a two-stage process. In the first stage, fast sorption on the external's sorbent surface occurs, while next slower diffusion to a particle interior along micropores wall takes place [137]. Nanoscale metal oxides possess higher adsorption ability and faster kinetics due to larger specific surface, shorter diffusion pathway to particle interior and higher number of active sites (i.e. corners, edges and other). For example, when the size of nanomagnetite particle is decreased from 300 to 11 nm, it is arsenic adsorption capacity increases more than 100 times [138]. Moreover, when particles' size is decreased to below 20 nm, the specific surface area increases and the ability of arsenic sorption by nanomagnetite of 11 nm diameter increases three times. This nanoscale effect is related to the change of magnetite surface structure related with the formation of new active adsorption sites [138].

Nanomaterials based on metal oxides are especially useful to remove heavy metals like arsenic, lead, copper, cadmium, nickel and possess much higher application potential in comparison with activated carbon [139]. Nanoparticles of a metal (hydro)oxide may also be impregnated on activated carbon or other porous materials to obtain simultaneous removal of metals (e.g. arsenic) and organic compounds, what favors their use in a point-of-use device [140].

Nanoadsorbents formed from metals oxides can be easily regenerated by a solution's pH change [139]. In many cases adsorption capacity of metal oxides, nanosorbents can be recovered even after regeneration and reuse cycles [141]. Relatively low costs of production of metal oxides based nanosorbents are also important. Hence, features like high adsorption ability, low cost, easy separation, and regeneration make metal oxide-based nanosorbents technologically and economically advantageous.

2.2.2.1. Iron oxides nanoparticles

The increasing interest in the use of iron oxides nanoparticles in water and wastewater treatment, especially in regarding toxic heavy metals removal, results from their unique physico-chemical properties like large specific surface, simple synthesis, and adsorption ability. The most commonly used iron oxides based nanosorbents are: non-magnetic goethite (α-FeOOH), hematite (α-Fe$_2$O$_3$), magnetic magnetite (Fe$_3$O$_4$) and maghemite (γ-Fe$_2$O$_3$) as well as hydrated iron oxides (HIO) [6–9,11,118]. Goethite and hematite possess a range of geochemical and ecological, important oxyanions and cations in their complex matrices, thus they are found as effective and cheap sorbents to removal of various contaminants [113]. Due to small size, however, their separation and recovery after wastewater treatment can be problematic. On the other hand, iron oxide-based nanoparticles like nano-maghemite (γ-Fe$_2$O$_3$) and nano-magnetite, despite their adsorption features possess also superparamagnetic properties. If the size of a magnetic particle is smaller than the critical value (ca. 40 nm), its separation and recovery in a low gradient magnetic field are easy [118]. Thus, iron oxide nanoparticles are efficient and promising nano-adsorbents for removal of a wide range of toxic contaminants from wastewater [6–9,11,118].

Nano-goethite reveals high adsorption capacity towards fluorides equal 59 mg/g and for the contaminant concentration decrease from 10.25 in raw stream to 0.5 mg/L in the treated stream [142]. Kinetics and mechanism of Cu^{2+} ions adsorption on nano-goethite indicate on the formation of Cu^{2+}/goethite complexes on adsorbent surface [143]. In case of hematite, which is also very reactive, maximum Cu^{2+} adsorption capacity reaches 84.46 mg/g. This result, however, is lower than the adsorption efficiency of nano-goethite (149.25 mg Cu(II)/g), even though both oxides reveal similar kinetics and adsorption mechanisms [144]. Adsorption of other metal ions (Pb(II), Cd(II), Cu(II) and Zn(II)) on nano-hematite have been investigated in the function of sorbent concentration, pH and temperature [144]. The results have shown complete removal of Pb, 94% removal of Cd, 89% removal of Cu and complete removal of Zn at sorbent dose equal 0.5 g/L. The impact of temperature on sorption has indicated on an endothermic reaction in case of Pb(II), Cu(II) and Cd(II), while in case of Zn(II) it is exothermic. Nano-goethite and nano-hematite are efficient and can be used in environmental re-cultivation processes. Nano-hematite has been found to be a good adsorbent for heavy metal ions, including arsenic (V) and chromium (VI) [143].

There are numerous research on the use of nano-maghemite and magnetite to heavy metals sorption, including arsenic, chromium, selenium, lead and nickel from synthetic (model) and natural aqueous systems [141].

Maghemite nanoparticles (10 nm) of surface 178 m^2/g reveal selective adsorption on harmful ions and fast process kinetics, while negligible effects of co-ions, for example, Na$^+$, Ca^{2+}, Mg^{2+}, Cu^{2+}, Ni^{2+}, NO$_3^-$, and Cl$^-$ is observed [141]. The adsorption mechanism is related to electrostatic attraction and ions exchange. Maghemite nanoparticles maintain initial adsorption capacity toward heavy metals removal even after six adsorption/desorption cycles [141]. Nano-magnetite is also used to remove contaminants like Cr(VI), Cu(II), Zn(II) and As(III/V), Se(IV) [145], as well as methylene blue and dichlorophenol [146] from aqueous solutions. Akhbarizadeh et al. [147] have investigated maghemite (γ-Fe$_2$O$_3$) nanoparticles as an adsorbent for removal of Cu(II), Ni(II), Mn(II), Cd(II) and Cr(VI) from water solutions. They have found that pH of a solution plays very important role in adsorption of Ni(II) Mn(II) and Cd(II), for which alkaline conditions are preferable (pH range of 8.5–10), while in case of Cu(II) and Cr(VI) acidic pH is required (pH 6.5 and 2.6). The process mechanism corresponds to monolayer adsorption according to Langmuir isotherm model with maximum capacity equal 24.21, 24.44, 23.47, 22.99 and 19.72 mg/g for Cr(VI), Cu(II), Mn(II), Ni(II) and Cd (II), respectively. Thus, the adsorption efficiency can be arranged in the following series: Cu (II) > Cr (VI) > Mn(II) > Ni(II) > Cd(II). The authors have also found that ionic radius and electronegativity play an important role in adsorption of the process. The smaller ionic radius and higher electronegativity of metal are, the higher adsorption efficiency is obtained. Nano-maghemite and magnetite can be produced in large amounts using relatively simple sol-gel

method, while the separation of magnetic adsorbent from treated water can be easily obtained by the simple application of magnetic field [141].

In oversaturated solutions, iron compounds hydrolyze, precipitate and aggregate as amorphous structures of high porosity finally composed of so-called hydrated iron oxides (HIO) [148], which reveal better ability of metal ions sorption than crystalline oxides like goethite. HIO possess active sites for sorption of various dissolved substances, which occur mainly due to surface complexation and ligands exchange. It has been found, that adsorption of Cu(II) or Pb(II) ions on amorphous HIO is independent of ionic strength, while it increases with pH increase [148]. Nano-iron hydroxide [α-FeO(OH)] is stable, mechanically resistant adsorbent of large specific surface, which enables adsorption of arsenic from wastewater and drinking water [149]. ArsenXnp (SolmeteX Inc., Philadelphia, PA, US), available on the market, is a hybrid medium to ion exchange, it contains nanoparticles of iron oxide and polymers and is very efficient in arsenic removal [113].

The functionalization of iron oxide nanoparticles with different ligands, like for example α-thio-ω(propionic acid), hepta-(ethylene glycol), mercaptobutyric acid, ethylene diamino-tetraacetic acid, L-glutathione, 2,3-dimercaptosuccinic acid [150] and 3-amino-propyl-trimethoxysilane [151] increases efficiency and selectivity of adsorption. It has been observed that after iron oxide nanoparticles surface modification, the adsorption of different metals from wastewater, that is, As(III), Pb(II), Cu(II), Co(II), Cr(III), Ni(II) and Cd(II) significantly increases [152].

Polymeric coatings are used to prevent aggregation of iron oxide nanoparticles and to improve their dispersion [150]. Khaydarov et al. [153] have used elastic layers integrated with various functional groups protecting iron oxide nanoparticles from damage. For example, magnetic Fe_3O_4 inoculated with polyethyleneimine (PEI) very efficiently adsorbs heavy metals like Cu^{2+}, Zn^{2+}, Cd^{2+} [154], while the use of polystyrene as a support for hydrated Fe_2O_3 enables adsorption of As(III) and As(V) ions [155]. Small organic particles are also widely used to stabilize nanoparticles. For example covalent immobilization of thiosalicylhydrazide on Fe_3O_4 NPs surface is efficient regarding the removal of heavy metal ions (Pb^{2+}, Cd^{2+}, Cu^{2+}, Zn^{2+}, and Co^{2+}) from industrial wastewaters [156]. Nano-Fe_3O_4 modified with basic Schiff's 6G rhodamine has revealed high selectivity and sensitivity toward Al^{3+} over other metal co-ions in aqueous solution [157]. To modify nano-Fe_3O_4, chemical compounds like EDTA, hydroxyapatite ($Ca_{10}(PO_4)_6(OH)_2$), silica dioxide ($Fe_3O_4@SiO_2$-NH_2), chitosan (chitosan/SiO_2/Fe_3O_4) and other can be used [11]. Such modified adsorbents have been tested in the removal of heavy metal ions from water.

2.2.2.2. Aluminum nanoparticles

Aluminum oxide reveals highest adsorption efficiency, when it appears in the form of γ-Al_2O_3, while when it is in α-Al_2O_3 form, the efficiency is poorer. Nano-γ-Al_2O_3 characterizes with large specific surface, high adsorption ability and satisfactory mechanical strength [158]. Nano-aluminum oxide produced by sol-gel method has been used in removal of Ni(II) from solutions [158] and it has revealed maximum efficiency equal to 96.6% at initial Ni(II) concentration 25 mg/L. Zhang et al [158] have shown, that nano-Al_2O_3 is an efficient adsorbent of Tl(III) ions, for which almost complete removal has been obtained in an aqueous solution of pH = 4.5. If nano-aluminum oxide reveals poor affinity to a certain metal, chemical or physical modification of γ-Al_2O_3 nanoparticles surface based on the introduction of functional groups containing oxygen and nitrogen is applied. For example nano-aluminum oxide coated with 2,4-dinitrophenylhydrazine (DNPH) immobilized on sodium dodecyl sulphate has been developed to remove cations like Cr(III), Pb(II) and Cd(II), and maximum adsorption capacity has reached 100.0, 83.33 and 10.0 mg/g, respectively [159].

2.2.2.3. Manganese oxide nanoparticles

Manganese oxide nanoparticles reveal excellent adsorption ability due to polymorphous structure and large specific surface area and are widely used to wastewater treatment to remove arsenic [159], other heavy metals (zinc(II), cadmium (II) and lead(II)) [6,160] and phosphates. The mechanism of adsorption of bivalent metal ions comprises two stages, that is, fast and reversible adsorption on an external surface, including its micropores followed by slow diffusion along the oxidized surface of walls of micropores. Mishra et al. [161] have found that hydrated manganese oxide is efficient in removal of Hg(II) ions from water solutions and maximum adsorption effectiveness is obtained at the contaminant's concentration range 10^{-8}–10^{-2} M, at temperature 298–328 K and pH 2.0–10.5.

2.2.2.4. Magnesium oxide nanoparticles

Magnesium oxide, in the form of nanospheres, is used to eliminate different types of toxic heavy metals from wastewater [6]. In order to improve adsorption ability of magnesium oxide, different methods of nanoparticle morphology change resulting in formation of three-dimensional structures of nano-bricks, nano-bars, nanotubes or nanorods have been used [6]. They have allowed for effective adsorption of lead(II) and cadmium(II) on magnesium oxide structures with mesopores [6].

2.2.2.5. Titanium oxide nanoparticles

TiO_2 nanoparticles combine functions of physical separation and catalyst reactivity toward contaminant degradation. A lot of effort has been given to develop inorganic photocatalytic nanoparticles comprised of nano-catalysts (nano-TiO_2 or modified nano-TiO_2) [162]. They are usually used to photochemical degradation of organic contaminants and as the adsorbent for the removal of heavy metals from water [163]. For example, nano-TiO_2 modified with thioglycolic acid and immobilized on silica gel as well as TiO_2 nanotubes have been used as adsorbents to remove ions like Ni^{2+}, Cd^{2+}, and Pb^{2+} from water [163], whereas TiO_2 nanoparticles (Anatase) immobilized on activated carbon have been applied to remove Cr(VI) [164]. Nanoparticles of sodium titanate are also regarded as an adsorbent and have been used to remove Cu^{2+} and Cd^{2+} from aqueous solution [164], while after immobilization on granulated activated carbon they

have been applied to remove Cu^{2+}, Cd^{2+}, Pb^{2+} and Zn^{2+} from water [165]. The composite of lignosulphonate and titanate has been used to adsorb Pb^{2+}, Cu^{2+} and Cd^{2+} ions [166,167].

TiO_2 is a photocatalytic semiconductor, which is the most often used in water/wastewater treatment, due to its biological and chemical neutrality and high oxidation potential. Photocatalysis with TiO_2 results in formation of highly reactive hydroxyl radicals ($OH^{\bullet}$), superoxide (O_2^-) and peroxide (O_2^{2-}) anions, which can decompose organic compounds at UV, visible or sunlight radiation [8]. Morphological structure, crystalline phase, structure damage prevention, energy gap and hydrophilicity can be adjusted by change of TiO_2 type, chain length or introduction of surface-active agent to production process [8]. Photo-activity of nano-TiO_2 can be increased by optimization of size and shape of nanoparticles, decrease of recombination of e^-/h^+ by noble metal addition and processing of surface aiming at contaminants adsorption increase. Among crystalline TiO_2 structures, rutile particles are the most stable at size range above 35 nm, while for particles smaller than 11 nm anatase is preferable [168]. If the size of particles is reduced to several nanometers, surface recombination is dominant and photocatalytic activity is reduced. The addition of noble metals may decrease e^-/h^+ recombination, as electrons excited by radiation migrate to a noble metal of lower Fermi level, while gaps maintain in TiO_2 [168]. Another area of research is dedicated to widening TiO_2 excitation spectrum by visible light. The general strategy relies on introduction of metals, dyes or semiconductors of narrow forbidden band or anions into nano-TiO_2, which results in formation of hybrid nano-particles or nano-composites [169]. Among these methods, introduction of anions (especially nitrogen-based ones) has been found to be the most beneficial solution regarding industrial application [169]. Photocatalysis with nano-TiO_2 is also more and more often used at activation with sunlight [169].

Photocatalytic inactivation of microorganisms is a complex process and its efficiency depends on type, concentration and physiological condition of microorganisms [170]. TiO_2 nanoparticles (Degussa P25, Essen, Germany) have been used in successful deactivation of different bacteria like *Escherichia coli*, *Pseudomonas aeruginosa*, *Salmonella typhimurium* and *Enterobacter cloacae* [169–171]. The use of TiO_2 nanoparticles (Degussa P25) to inactivation of bacteria (*E. coli*, *Pseudomonas aeruginosa*), fungi (*Candida albicans*, *Fusarium solani*), protozoa (stadium trophozoite stage of *Acanthamoeba*), spores (*Bacillus subtilis*) and cysts at sun radiation is also discussed in the literature [8].

Photocatalysis with nano-TiO_2 is also widely used in wastewater treatment to decompose and mineralize various contaminants and micropollutants like endocrine disruptors, cyanotoxins, antibiotics, pesticides, dyes, polymers, phenolic contaminants, aldrin, polychlorinated bisphenols and other. Rahman et al [172] have investigated kinetics of degradation of two pesticides, that is, dichlorvos and phosphamidon using Degussa 25 (commercially available TiO_2 nanoparticles) and they have found that addition of acceptors like hydrogen peroxide (H_2O_2) increases contaminants degradation rate. Solar photocatalysis has been also successfully applied to degradation of aldrin and its three derivatives that is, dieldrin, chlordane and 1,2-hydroxydieldrin [172]. Dichlorvos, which, due to its toxicity, is classified as restricted use pesticide, is efficiently degraded by photocatalysts like TiO_2 and ZnO [172].

2.2.2.6. Zinc oxide nanoparticles

Zinc oxide (ZnO) has been most often used as an adsorbent for H_2S elimination [173]. Porous nano-ZnO plates of pores diameter 5–20 nm and large specific surface (147 m^2/g) have also revealed strong and selective adsorption of cations of toxic metals [174], including Cu(II) with efficiency above 1,600 mg/g. Such the high adsorption capacity results from the high number of polar active sites of nano-plates able to bond hydrated Cu(II) ions by formation of Cu–O–Cu bonds on pores' walls [174]. Nano-ZnO can also effectively remove Cd(II) and Hg(II) ions with maximum capacity equal to 387 and 714 mg/g, respectively [174]. Hydroxyl groups on nano-ZnO surface have been found to play an important role in adsorption of various heavy metals.

Zinc oxide (ZnO) nanoparticles, next to TiO_2, have also been recognized as an efficient and promising photocatalyst to wastewater treatment because they can be activated by visible light (<450 nm) [165]. Photocatalytic features of nano-ZnO are comparable to ones of TiO_2 due to the fact, that their energy bands are practically identical, while nano-ZnO is cheaper and adsorbs wider spectrum of sunlight in comparison with other metals oxide semiconductors [175]. The main disadvantages of nano-ZnO are large difference in energy band and photocorrosion resulting from fast regrouping of photo-generated charges, which decreases photocatalytic properties [175]. The introduction of other metals to nano-ZnO structure is one of the methods used for the improvement of the material photocatalytic ability. Cationic and anionic injections of rare earth metals have been investigated regarding improvement of nano-ZnO photocatalytic ability [176,177]. Moreover, some research suggests, that modification of nano-ZnO with semiconductive materials like graphene oxide [178], tin(IV) oxide [179], cadmium oxide [180], titanium dioxide [181] and cerium(IV) oxide [177] is practical method of zinc oxide nanoparticles photo-degradation ability increase.

Table 7 summarizes the results of the research on various metal ions removal from wastewater using inorganic nanomaterials.

2.3. Nanocomposite materials

Nanoparticles of large specific surface areas used in water and wastewater treatment possess some limitations, which include aggregation, release to environment and potentially harmful effect on ecosystems and human bodies [6,8]. These issues can be solved or minimized by formation of nanocomposite materials. Nanocomposites are multiphase materials, in which a minimum one phase has dimensions in the range of 10–100 nm. Their classification can be made either according to matrix material (inorganic or polymeric) or according to dispersed phase-type (CNT, graphene, metals, metal oxides) [6,8]. Nanocomposite materials integrate functional features of nanoparticles and matrices and reveal huge potential for industrial-scale applications. The examples of nanocomposites have been discussed in detail in chapters 2.1 and 2.2.

Table 7
Heavy metals adsorption capacities revealed by selected metal oxide nanomaterials

Adsorbents	Metal ions	Sorption capacity	Experiment conditions	Reference
Goethite (α-FeOOH)	Cu(II)	100%	pH = 6	[182]
	F$^-$	59 mg/g	pH = 7	[142]
Hematite (α-Fe$_2$O$_3$)	Pb(II)	100%	pH = 8	[144]
	Cd(II)	94%		
	Cu(II)	89%		
	Zn(II)	100%		
Maghemite (γ-Fe$_2$O$_3$)	Cr(VI)	24.21 mg/g	Dose 2 g/L	[147]
	Cu(II)	24.44 mg/g	Metal conc. 2–250 mg/L	
	Mn(II)	23.47 mg/g	Temp. 298 K	
	Ni(II)	22.99 mg/g	Time 15 min	
	Cd(II)	19.72 mg/g		
Magnetite (Fe$_3$O$_4$)	Se(IV)	Se reduced to <5 from 100 µg/L	pH = 2–4	[183]
Polymer modified Fe$_3$O$_4$	Cd(II)	29.6 mg/g	Dose 1.0 g/L	[150]
	Pb(II)	166.1 mg/g	Metal conc. 20–450 mg/L	
	Zn(II)	43.4 mg/g	Temp. 298 K	
	Cu(II)	126.9 mg/g	pH = 5.5; Time 45 min	
Na lauryl sulfate modified Fe$_3$O$_4$	Cr(VI)	30.7 mg/g	Dose 2 g/L; metal conc. 5–300 mg/L; pH = 4.0; temp. 293 K	[184]
EDTA modified Fe$_3$O$_4$	Cu(II)	46.27 mg/g	Dose 0.5 g/L; metal conc 1.0–6.0 mg/L; pH = 6.0; temp. 298 K	[185]
Fe3O4@SiO2–NH2	Pb(II)	243.9 mg/g	Dose 1.2/g/L; pH 7.0; metal conc. 2–200 mg/L	[186]
Magnetite nanorod	Fe(II)	127.0 mg/g	Dose 1.0 g/L; metal conc. 10–200 mg/L; pH = 5.5; temp. 298 K; time 60 min	[187]
	Pb(II)	112.9 mg/g		
	Zn(II)	107.3 mg/g		
	Ni(II)	95.4 mg/g		
	Cd(II)	88.4 mg/g		
	Cu(II)	76.1 mg/g		
Hydrous ferric oxide (HFO)	F	6.71 mg/g; 3.26 – bed column	pH = 6.5	[188]

(Continued)

Table 7   Continued

Adsorbents	Metal ions	Sorption capacity	Experiment conditions	Reference
Nano-Al$_2$O$_3$	Pb(II)	100 mg/g	pH = 5.5	[159,189,190]
	Cd(II)	83.3 mg/g		
	Cr(III)	100 mg/g		
	Cr((VI)	3.95–8.56 mg/g		
	Ni(II)	30.82 mg/g		
γ-Al$_2$O$_3$	Pb(II)	125.0 mg/g	Dose 4.0 g/L; time 180 min; metal conc. 25–150 mg/L; temp. 298 K; pH 4.0	[191]
	Ni(II)	83.33 mg/g		
	Zn(II))	58.82 mg/g		
TiO$_2$	Pb(II)	99.9%	pH = 8	[109]
	Cd(II)	96.2%		
	Zn(II)	98.2%		
ZnO	Zn(II)	357 mg/g	pH=8	[175]
	Cd(II)	387 mg/g		
	Hg(II)	714 mg/g		
Precipitated nano-NiO Organic extraction	Pb(II)	56.24 mg/g	Dose 1.0 g/L; pH 5.8; temp. 298 K; time 120 min	[192]
		21.55 mg/g		
Nano-MnO$_2$	Cu(II)	2.439 mg/g	Dose 10 g L^{-1}; pH = 5.0; temp. 298 K	[193]
	Ni(II)	5.555 mg/g		
	Co(II)	0.200 mg/g		
	Zn(II)	6.250 mg/g		
Nano-CuO	As(V)	18.21 mg/g	Metal conc. 6–60 mg/L; pH 7.0; temp. 298 K; time 1,440 min	[194]
Nano-CuO	Cr(VI)	15.63–18.52 mg/g	Dose 1.6 g/L; temp. 298–318 K; pH = 5.8; time 180 min; metal ion conc. 10–150 m/L	[195]
ZnO@SiO$_2$@Fe$_3$O$_4$/C	Pb(II)	94.3 mg/g	Dose 1.2 g/L; metal conc. 2–200 mg/L, pH =7.0; temp 298 K	[196]
	As(V)	23.6 mg/g		
CuFe$_2$O$_4$	Cd(II)	17.54 mg/g	Dose 5.0 g/L; pH = 6.0; time 20 min; temp. 318 K	[197]

Among various nanocomposites, polymeric nanocomposites (PNCs) have become a subject of some research and development actions due to many advantageous features such as film formation, dimensional changeability, and activation by functionalization [198]. PNCs are prospective materials for water and wastewater treatment, as they possess properties of nanoparticles and polymeric matrices [6,8,199]. They can be obtained by using one among two main methods, that is, direct mixing or in-situ synthesis [199,200]. The first method relies on the direct introduction of functional nanoparticles or their injection to a polymer, while the second method is based on initial saturation of polymer pores with nanoparticles precursors followed by in-situ synthesis by precipitation and nucleation with dedicated initiators. Another method of in-situ synthesis is the addition of functional nanoparticles during polymerization of monomers (Fig. 5).

Among commonly used polymeric matrices one can find alginate [201], macroparticles (e.g. polypyrrole) [202], polyaniline [203], porous resins and ion exchangers [204]. One of the most often used polymeric support is cross-linked polystyrene-based ion exchanger. Its surface is suitable to be modified with positively or negatively charged functional groups ($-SO_3^{-2}$ and $-CH_2N^+(CH_3)_3$), and it allows for easy permeation and dispersion of nanoparticles precursors (such as Zr^{4+} or $FeCl_4^-$) to its pores interior [205]. These mentioned nanocomposites possess a large removal potential of contaminants present in water and wastewater. Moreover, the stability of the immobilized nanoparticles is much higher in comparison with non-immobilized ones.

Other types of polymeric matrices are biopolymers like chitosan and cellulose, which appear commonly in nature and are relatively eco-friendly [206]. Cellulose characterizes with good chemical and mechanical stability and hydrophilicity due to tightly packed, ordered and hydrogen-bonded particles, which guarantees resistance to swelling [206]. Nanoparticles of cellulose (NCs) also reveal adsorption and ion exchange properties and are very similar to polymeric nanocomposites [206]. Another natural composite support is chitosan [207], which characterizes with high reactivity, excellent chelating properties and chemical stability [207]. Amine and other functional groups of chitosan act as active sites for adsorption of contaminants from water [207]. Cross-linked

chitosan is insoluble even at low pH, thus it can be used in a wide pH range [207]. The high adsorption efficiency of chitosan-based nanoparticles regarding different contaminants present in water and wastewater has been widely discussed in the literature [207].

Inorganic nanocomposites' supports cover mainly activated carbon, CNT as well as natural minerals like zeolite, biochar, and clays.

Activated carbon (AC) is a conventional adsorbent commonly used to water and wastewater treatment and it can be used as an excellent support for nanoparticles [208]. As examples, AC composites with immobilized nanoparticles of oxy-hydroxy iron (As (V) adsorption) [209], nano-ZnO (Pb(II) adsorption) [210] or magnetite (Fe_3O_4) (aromatic contaminants adsorption) [211] can be mentioned.

CNTs nanocomposites (CNTs-NCs) cover materials, in which CNTs are the basic component [212]. Poly-1,8-diaminonaphthalene/MWCNT-COOH hybrid material can be an adsorbent for separation of trace amounts of Cd(II) and Pb(II) (adsorption capacity of Cd(II) and Pb(II) – 101.2 and 175.2 mg/g, respectively) [213]. Konicki et al. [214] have used M-MWCNTs–Fe_3C (M-MWCNTs-ICN) to remove Red 23 from an aqueous solution with maximum capacity of 85.5 mg/g. Other examples of CNTs based nanocomposites are discussed in chapter 2.1.1.

Zeolites are widely used as an adsorbent, ion exchange material and catalyst due to low costs and unique internal structure, which possesses many active sites. Mthombo et al. [215] have investigated adsorption of Cu(II), Pb(II) and Co(II) on vinyl-ethylene-clynoptylolyte acetate nanocomposite, Khatamian and Alaji [216] have prepared nanocomposite of zeolite and ZnO for adsorption of 4-nitrophenol (4-NPh), while Chong et al. [217] have synthesized nanocomposite of TiO_2-zeolite to industrial dyes removal.

Biochar is commonly available and cheap material produced by biomass pyrolysis in anaerobic conditions. Nanocomposites containing biochar are usually obtained from biomass initially enriched with nanoparticles precursors or by direct impregnation of nanoparticles after pyrolysis [218]. As examples of such materials, one should mention γ-Fe_2O_3/biochar nanocomposites, which reveal good adsorption of As(V) ions [219]. CNT-biochar nanocomposites of large specific surface area (359 m^2/g) have been used
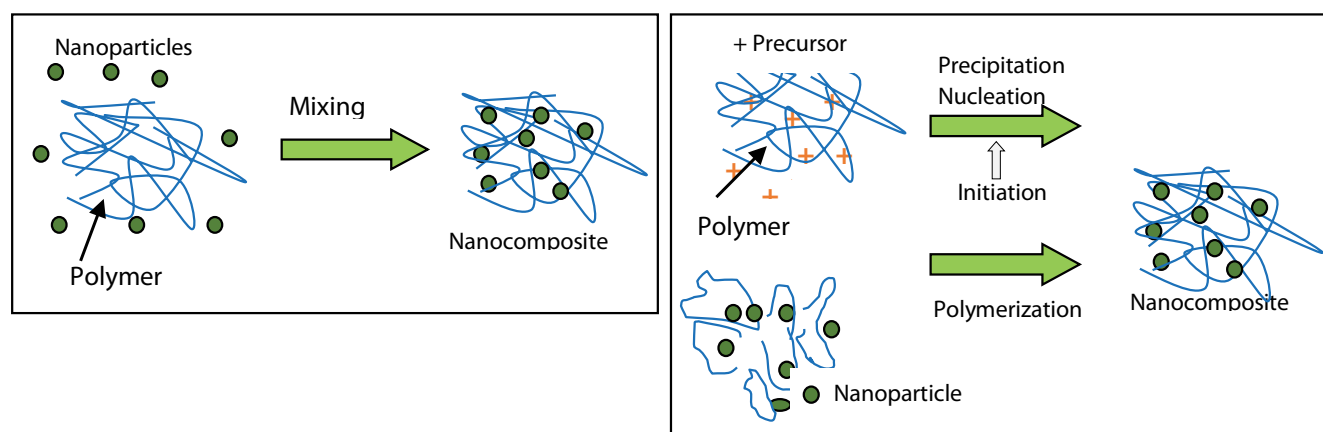

Fig. 5. Methods of production of polymeric nanocomposites.

to dyes adsorption [220], while biochar/MgO adsorbents have revealed very high adsorption capacity of phosphates (835 mg/g) [221].

Polymeric nanocomposites based on clays (CPNs) are mixtures of polymers and inorganic clay materials, in which inorganic, as well as organic nanoparticles, are present. CPNs reveal good mechanical and chemical stability, thermal resistant, large specific surface, and limited gas permeability. Various CPNs are widely used to remove organic and inorganic micropollutants like Co(II), Zn(II), Se(IC) and atrazine [222]. CPNs of Cu/polyethylene/montmorillonite type shows strong antibacterial effect toward *E. coli* [223].

In recent years, nanocomposites have appeared as a realistic alternative for activated carbon to water and wastewater treatment. Large specific surface, excellent mechanical stability, surface modification possibility and pore size distribution make this material preferable in reference to many other adsorbents [11].

3. Mechanism of adsorption

In order to understand an adsorption mechanism, a combination of experimental studies and theoretical calculations is needed. The characterization of the adsorbent by Brunauer–Emmett–Teller surface area, Fourier-transform infrared spectroscopy (FTIR), transmission electron microscopy, scanning electron microscopy with energy-dispersive X-ray spectroscopy and X-ray photoelectron spectroscopy can provide some explanations on the adsorption pathways [11]. The prediction of ions and organic contaminants adsorption on nano-adsorbents is not simple, and different possible interactions between them have been proposed. Hydrophobic interactions, van der Waals forces, π–π stacking, hydrogen bonding, complexation, and electrostatic interactions might act simultaneously or individually [88].

The process of solute adsorption is normally considered to be a physical process, in which van der Waals forces are usually dominant [88]. Physical adsorption is a kind of adsorption, which attaches the target substance to an adsorbent as a result of hydrogen bonding, van der Waals forces, electrostatic forces, and hydrophobic interactions. Physical adsorption can also be referred to as physisorption. Unlike in physical adsorption, if the molecular forces during the process of adsorption result in an electron exchange reaction, it means that a chemical adsorption occurs between the contaminant molecules and the solid surface of the nano-adsorbents [88]. Chemical adsorption, also known as chemisorption, involves a chemical reaction between the adsorbent surface and the adsorbate.

Kinetic models can give information related to adsorption pathways and probable mechanisms involved [11]. Adsorption kinetic also controls the rate of adsorption, which determines the time required for reaching equilibrium of the adsorption process; this is one of the most valuable information for adsorption system design. In liquid-phase adsorption, the rate can be determined by the following steps [224,225]:

- adsorbate transport from the bulk of the solution to the liquid film surrounding the solid adsorbent,
- of adsorbate across the liquid film surrounding of the solid adsorbent to the solid surface,
- of adsorbate from the liquid film into the pores of the solid adsorbent via intraparticle diffusion,
- adsorption of the adsorbate on the adsorbent surface either by chemical reaction or by physical processes,
- desorption of the adsorbate from the solid adsorbent surface (in case of reversible adsorption).

Generally, the overall rate of the adsorption is controlled by the slowest step. Many researchers have observed that most of the adsorption processes of heavy metals on nanomaterials follow pseudo-second-order kinetics rather than first-order kinetics [11].

Experimental and adsorption isotherm models and the instrumental methods can also give valuable information to determine adsorption mechanisms. The equilibrium distribution of adsorbate in the solid surface of adsorbent is normally measured as the amount of a substance adsorbed per unit mass of an adsorbent at equilibrium and the adsorbate concentration in the liquid phase at equilibrium. Data obtained from an adsorption isotherm model can give valuable information regarding adsorption phenomenon and is crucial for designing an economically viable commercial treatment system [226]. In the literature, many different types of isotherm models have been used over the years, among which some have been based on theoretical background, while others have been determined empirically [227]. The isotherm models used to describe the adsorption equilibrium are Langmuir, Freundlich, Dubinin–Radushkevich (D–R), Temkin, Elovich, and Redlich–Peterson (R–P) models [88]. Additionally, D–R isotherm model allows determining the mean energy of adsorption (E). If E is <8 kJ/mol, then physisorption is the dominant adsorption mechanism, while if E is in the range 8–16 kJ/mol, then adsorption is most probably follows chemisorption mechanism [228]. Researches dedicated to the application of various isotherm models are still inadequate, especially regarding adsorption on nanomaterials. The published references prefer two-parameter models, especially the Langmuir and Freundlich models because they can be simply linearized [69].

The thermodynamic parameters of adsorption, that is, the standard Gibbs free energy change (ΔG), the enthalpy change (ΔH), and the entropy change (ΔS) can be computed according to thermodynamic laws through the adequate equations. Each thermodynamic parameter has its physical sense in the adsorption system. ΔG can be regarded as the minimum isothermal work required to load a certain amount of adsorbate on the adsorbent surface. ΔH shows the heat effect of the adsorption system, while ΔS reflects the packing manner of adsorbate molecules on the surface of adsorbent [69,229]. The negative value of ΔG reveals that the adsorption process is feasible and spontaneous. The negative value of ΔH infers that the adsorption reaction is exothermic in nature and energetically stable, whereas the positive value suggests that the adsorption is endothermic and is supported by the increasing adsorption of metal ions with increasing temperature. The positive ΔS value indicates the increased randomness at the solid/solution interface during the adsorption process.

The electrostatic interaction between metal ions and the negatively charged surface of the adsorbate accompanied by

complexation and ion exchange are the primary mechanisms for adsorption of metals [69,147,229,230]. Electrostatic interactions occur between metal cations and negative surface charge and/or p electrons of the adsorbent [74,231]. The electron donor–acceptor complexes are formed by a coordination bond between the unshared electron pair of the adsorbent and an electron-deficient atom of a metal ion [74]. Functional groups of nanomaterials' surface for complexation and ion exchange are found to be hydroxyl, carboxylic, lactonic, phenolic, imine, amine and sulfonated groups [232–237].

For example, during examining adsorption of Cr(VI) on chitosan–magnetite adsorbent, authors have stated that Cr(VI) exists in aqueous solution in various anionic forms, and thus they can easily electrostatically interact with the protonated amine, hydroxyl, and carboxylates groups of chitosan [231]. Then Cr(VI) replaces H^+ ions by ion exchange process on the Fe_3O_4 surface. Similar explanation for adsorption of Cu(II), Ni(II), Mn(II), Cd(II), and Cr(VI) on maghemite nanoparticles (γ-Fe_2O_3) and $CuFe_2O_4$ has been reported by Akhbarizadeh et al. [147], Babaei et al. [184] and Tu et al. [197]. Moreover, Ashour et al. [238] have stated that electrostatic attraction is a primary mechanism for adsorption of La(III), Nd(III), Gd(III), and Y (III) ions on composite nanoadsorbent Cys-Fe_3O_4. Complexation, due to electrostatic interaction, is also a mechanism for adsorption of metals ions (e.g. Pb(II)) on amino-functionalized magnetic nanoadsorbent (MNPs-NH_2) [239]. Metal ions form stable complexes with EDTA functionalized magnetite nanoparticles due to electrostatic interaction [185].

Electrostatic interaction followed by ion-exchange mechanism are also the only pathways for adsorption of Cr(VI), Co(II), Ni(II), Cd(II), Pb(II), Zn(II) and Cu(II) ions on non-iron adsorbents (nano-γ-Al_2O_3, nano-MnO_2, nano-ZnO) from water [160,175,240]. Electrostatic attraction along with surface complexation is also responsible for adsorption of metals on nano-Al_2O_3 [189].

Electrostatic interaction is also responsible for adsorption of metal ions on graphene, single- and multi-walled CNTs [11]. This is due to the increase in the amount of oxygen-containing functional groups, like –COOH, –OH, and –C=O, on the surface of the carbon nanomaterials. The modification process increases the surface negativity of such a nanoadsorbent, and oxygen atoms in the functional groups can easily interact with metal ions causing their surface adsorption [241]. The presence of –C=O, C–O–C≡ and/or O–C=O groups at carbon edge sites, pyridinic nitrogen, and sp^2-nitrogen atoms bonded to C atoms plays a significant role in higher metal adsorption by electrostatic interaction [242]. The functional groups or molecules can be grafted onto the nano-adsorbents surface through techniques such as carboxylation, sulfonation, oxidation, phosphorylation, esterification, etherification and amidation. These materials include organic molecules (e.g., ethylenediaminetetraacetic acid and cyanobacterium metallothionein), polymers or copolymers (e.g., polyaniline, polypyrrole, chitosan, etc.), inorganic materials (e.g., Fe_3O_4, MnO_2, CdS, and Ag), and acids (i.e., sulfuric acid and phosphate) [69].

The adsorption of Ni(II) on graphene nanosheet/δ-MnO_2 has also been reported to follow electrostatic mechanism [243]. Pb(II) has shown preference for –N= groups rather than –NH in the poly(o-phenylenediamine)/reduced graphene oxide composite (PoPD/RGO) for electrostatic interaction [244]. This shows that the functional groups present on the surface of nanoadsorbents play an important role in the adsorption of heavy metals from water.

Electrostatic interaction and complexation are also responsible for the adsorption of metals on the nanocomposite adsorbents. For example, the TiO_2-acrylamide nanocomposite adsorption mechanism of Cd has been described as a chemical interaction between R-NH_2Cd^{2+} and Cd–O on the nanocomposite [245]. The functional groups like –COOH, –OH, or –C=O present on the surface of nanosized carbon immobilized Ca-alginate beads (NCBs) can electrostatically interact with the Co(II) and Ni(II) [246]. The functional groups present in nanocellulose are responsible for providing the binding sites for Cu(II) and Ni(II) through electrostatic interaction [247]. Khan et al. [248] have also reported that functional groups, such as –C=O, C–H, O–H, and C–O and along with Zr–O bond on nanohybrid cellulose/ZrO_2 adsorbent form the complex with Ni(II). On the other hand, ion-exchange, complexation, as well as electrostatic attraction is the key factor for the adsorption of Cr(VI) on hydroxyapatite-based chitin (n-HApC) and chitosan (n-HApCs) hybrid composites [249]. El-kafrawy et al. [250], through FTIR and XPS analysis, have noted that the oxygen atoms on the polymeric composite are the main binding sites for metal to form surface complexes by electrostatic interaction.

Adsorption studies at different pH can also provide additional information on electrostatic or covalent interactions between an adsorbate and an adsorbent. This is because at different pH, the metal may appear at different ionic forms and the zeta potential data of the adsorbent provide information regarding the surface charge of the adsorbent in different pH. Therefore, by observing the adsorption trend, the nature of bond formation between absorbent and adsorbate can be predicted [251].

Fig. 6 presents mechanisms and pathways of the removal of various species by the adsorption [9,11,13,113,117 and 118].
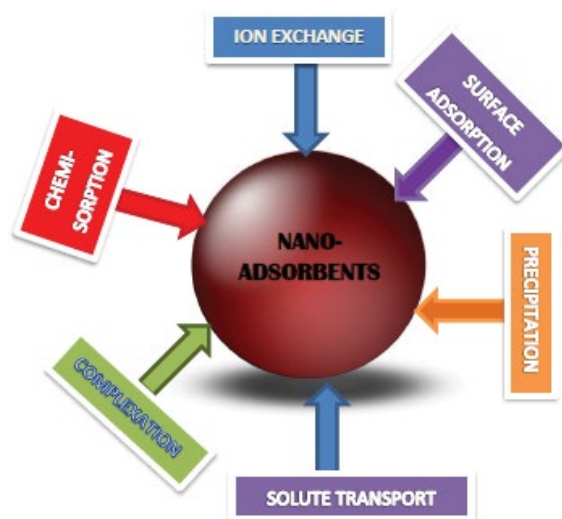
Fig. 6. Schematic illustration of various mechanisms of adsorption of metal ions by nanoparticles.

Therefore, it can be seen that the indication of the adsorption mechanism is not an easy task and researcher need to obtain various information, both experimentally and with the help of theoretical calculations before they can propose any plausible mechanism for a given adsorption process.

4. Conclusion

Many researches on the use of nanomaterials to adsorption of metal ions and other contaminants have been performed. The most investigated and preferable materials are nanosorbents made from metal oxides, especially iron-based ones, and CNTs. Chemical modification often changes character of nanosorbents surface, which significantly improves adsorption abilities. Recently, an increasing interest in removal of metal ions from aquatic environment through composite nanoadsorbents has been observed, due to their potential use in the industrial scale. Properties of nanocomposites surface can be modified regarding specific requirements, what assures their proper selectivity.

Despite intensive research, there are no reports on commercial use of nanomaterials to water and wastewater treatment. As the reason, one should mention difficulties in regeneration of saturated nanoparticles and their potential toxicity to living organisms. It limits the replacement of low-cost conventional adsorbents with nanoadsorbents in water and wastewater treatment, especially because conventional adsorbents can be used to remove almost all contaminants, which usually appear in aqueous streams. On the other hand, the comparison of adsorption properties of conventional adsorbents and nanoadsorbents regarding contaminants removal indicates on benefits of nanomaterials due to higher efficiency, shorter contact time, faster kinetics, lower doses, usability in wide pH range and removal of trace amounts of toxic heavy metals. Hence, despite some limitations, nanoadsorbents seem to be a good solution for water and wastewater treatment. However, some issues like preparation of nanoparticles from biodegradable materials, their efficient handling without environmental hazards and optimization of treatment techniques in the pilot and commercial scale need to be solved. The evaluation of economy and energy consumption for the use of some nanoadsorbents in wastewater treatment has been discussed in many papers, which shows that nanoadsorbents offer more efficient water treatment technology than other adsorbents [109]. The hazardous effect of nanoparticles regarding the environment, but also to human health, known as nanotoxicity, is also an open topic. Some information on the toxicity of metal oxides nanoparticles (aluminum oxide, titanium oxide, zinc oxide) and CNTs [10] in regard to living organisms can be found in the literature. The high chemical reactivity of nanoparticles results from the generation of free radicals, thus their presence in living organisms can cause oxidative stress and inflammation. Hence, efficient and safe methods of nanoparticles utilization need to be urgently developed.

Based on results of many adsorption research discussed in this paper it can be stated, that nanoparticles can be potential, stabile and effective substitute of conventional sorbents, especially in the removal of heavy metals from water and wastewater.

References

[1] X. Tian, J. Sarkis, Y. Geng, Y. Qian, C. Gao, R. Bleischwitz, Y. Xu, Evolution of China's water footprint and virtual water trade: a global trade assessment, Environ. Int., 121 (2018) 178–188.

[2] World Health Organization, Progress on drinking water and sanitation: 2012 update. UNICEF, WHO Geneva, (2012).

[3] S. Baruah, M. N. Khan, J. Dutta, Nanotechnology in water treatment. In: Lichtfouse E, Schwarzbaur J, Robert D (eds.) Pollutants in buildings, water and living organisms. Environ. Chem. for a sustainable world, Springer International Publishing, Switzerland, vol. 7 (2015) pp. 51–84.

[4] J. Nawrocki, Water Treatment. Chemical and Biological Processes, Wydawnictwo Naukowe PWN, Warszawa, Poland, 2010 (in Polish).

[5] M. Bodzek, Membrane separation techniques – removal of inorganic and organic admixtures and impurities from water environment – review, Arch. Environ. Prot., 45 (2019) 4–19.

[6] L. Madhura, S. Singh, S. Kanchi, M. Sabela, K. Bisetty, Nanotechnology based water quality management for wastewater treatment, Environ. Chem. Lett., 17 (2018) 65–121.

[7] M. Bodzek, K. Konieczny, M. Rajca, Membranes in water and wastewater disinfection – review, Arch. Environ. Prot., 45 (2019) 3–18.

[8] Y. Zhang, B. Wu, H. Xu, H. Liu, M. Wang, Y. He, B. Pan, Nanomaterials-enabled water and wastewater treatment, NanoImpact, 3–4 (2016) 22–39.

[9] F. Lu, D. Astruc, Nanomaterials for removal of toxic elements from water, Coord. Chem. Rev., 356 (2018) 147–164.

[10] M. Kamali, K.M. Persson, M.E. Costa, I. Capela, Sustainability criteria for assessing nanotechnology applicability in industrial wastewater treatment: current status and future outlook, Environ. Int., 125 (2019) 261–276.

[11] G.K. Sarma, S.S. Gupta, K.G. Bhattacharyya, Nanomaterials as versatile adsorbents for heavy metal ions in water: a review, Environ. Sci. Pollut. Res., 26 (2019) 6245–6278.

[12] I. Ali, New generation adsorbents for water treatment, Chem. Rev., 112 (2012) 5073–5091.

[13] M. Khajeh, S. Laurent, K. Dastafkan, Nanoadsorbents: classification, preparation, and applications (with emphasis on aqueous media), Chem. Rev., 113 (2013) 7728–7768.

[14] D. Ren, J.A. Smith, Retention and transport of silver nanoparticles in a ceramic porous medium used for point-of-use water treatment, Environ. Sci. Technol., 47 (2013) 3825–3832.

[15] S. Wang, C.W. Ng, W. Wang, Q. Li, Z. Hao, Synergistic and competitive adsorption of organic dyes on multiwalled carbon nanotubes, Chem. Eng. J., 197 (2012) 34–40.

[16] S.D. Lakshmi, P.K. Avti, G. Hegde, Activated carbon nanoparticles from biowaste as new generation antimicrobial agents: a review, Nano-Struct. Nano-Objects, 16 (2018) 306–321.

[17] N. Bagheri, J. Abedi, Preparation of high surface area activated carbon from corn by chemical activation using potassium hydroxide, Chem. Eng. Res. Des., 89 (2009) 1059–1064.

[18] K.V. Gupta, D. Mohan, S. Sharma, M. Sharma, Removal of basic dyes (rhodamine B and methylene blue) from aqueous solutions using bagasse fly ash, Sep. Sci. Technol., 35 (2000) 2097–2113.

[19] S.M. Anisuzzaman, C.G. Joseph, Y.H. Taufiq-Yap, D. Krishnaiah, V.V. Tay, Modification of commercial activated carbon for the removal of 2,4-dichlorophenol from simulated wastewater, J. King Saud Univ. Sci., 27 (2015) 318–330.

[20] O.A. Habeeb, K. Ramesh, G.A.M. Ali, Low-cost and eco-friendly activated carbon from modified palm Shell for hydrogen sulfide removal from wastewater: adsorption and kinetic studies, Desal. Water Treat., 84 (2017) 205–214

[21] O.A. Habeeb, R. Kanthasamy1, G.A.M. Ali, R.M.Yunus, Experimental design technique on removal of hydrogen sulfide using Cao-eggshells dispersed onto palm kernel shell activated carbon: experiment, optimization, equilibrium and kinetic studies, J. Wuhan Univ.Technol.-Mater. Sci. Ed., 32 (2017) 305–320.

[22] M. Bahgat, A. Farghali, W. El Rouby, M. Khedr, Synthesis and modification of multi-walled carbon nano-tubes (MWCNTs) for

water treatment applications, J. Anal. Appl. Pyrolysis, 92 (2011) 307–313.

[23] R. Das, S.B.A. Hamid, E.M. Ali, A.F. Ismail, M.S.M. Annuar, S. Ramakrishna, Multifunctional carbon nanotubes in water treatment: the present, past and future, Desalination, 354 (2014) 160–179.

[24] K. Yang, B.S. Xing, Adsorption of organic compounds by carbon nanomaterials in aqueous phase: Polanyi theory and its application, Chem. Rev., 110 (2010) 5989–6008.

[25] X. Wang, J. Lu, B. Xing, Sorption of organic contaminants by carbon nanotubes: influence of X adsorbed organic matter, Environ. Sci. Technol., 42 (2008) 3207–3212.

[26] M. Rajabi, B. Mirza, K. Mahanpoor, M. Mirjalili, F. Najafi, O. Moradi, H. Sadegh, R. Shahryari-Ghoshekandi, M. Asif, I. Tyagi, Adsorption of malachite green from aqueous solution by carboxylate group functionalized multi-walled carbon nanotubes: determination of equilibrium and kinetics parameters, J. Ind. Eng. Chem., 34 (2016) 130–138.

[27] V.K. Gupta, O. Moradi, I. Tyagi, S. Agarwal, H. Sadegh, R. Shahryari-Ghoshekandi, A.S.H. Makhlouf, M. Goodarzi, A. Garshasbi, Study on the removal of heavy metal ions from industry waste by carbon nanotubes: effect of the surface modification: a review, Crit. Rev. Env. Sci. Technol., 46 (2016) 93–118.

[28] H. Sadegh, G.A.M. Ali, H.J. Nia, Z. Mahmoodi, Nanomaterial Surface Modifications for Enhancement of the Pollutant Adsorption from Wastewater, R. Nazir, Ed., Nanotechnology Applications in Environmental Engineering, IGI Global, Hershey, 2019, pp. 143–170.

[29] E. Roumeli, D.G. Papageorgiou, V. Tsanaktsis, Z. Terzopoulou, K. Chrissafis, A. Avgeropoulos, D.N. Bikiaris, Amino-functionalized multiwalled carbon nanotubes lead to successful ring-opening polymerization of poly(ε-caprolactone): enhanced interfacial bonding and optimized mechanical properties, ACS Appl. Mater. Interfaces, 7 (2015) 11683–11694.

[30] C.L. Ngo, Q.T. Le, T.T. Ngo, D.N. Nguyen, M.T. Vu, Surface modification and functionalization of carbon nanotube with some organic compounds, Adv. Nat. Sci.: Nanosci. Nanotechnol., 4 (2013) 035017–035022.

[31] G.A.M. Ali, E.Y.L. Teo, E.A.A. Aboelazm, H. Sadegh, A.O.H. Memar, R. Shahryari-Ghoshekandi, K.F. Chong, Capacitive performance of cysteamine functionalized carbon nanotubes, Mater. Chem. Phys., 197 (2017) 100–104.

[32] J.M. Ngoy, S.E. Iyuke, W.E. Neuse, C.S. Yah, Covalent functionalization for multi-walled carbon nanotube (f-WCNT)-folic acid bound bioconjugate, J. Appl. Sci., 11 (2011) 2700–2711.

[33] K.T. Kim, W.H. Jo, Noncovalent functionalization of multiwalled carbon nanotubes using graft copolymer with naphthalene and its application as a reinforcing filler for poly(styrene-co-acrylonitrile), J. Polym. Sci., Part A: Polym. Chem., 48 (2010) 4184–4191.

[34] H. Sadegh, G.A.M. Ali, A.S.H. Makhlouf, K.F. Chong, N.S. Alharbi, S. Agarwal, V.K. Gupta, MWCNTs-Fe_3O_4 nanocomposite for Hg(II) high adsorption efficiency, J. Mol. Liq., 258 (2018) 345–353.

[35] C.L. Chiang, C.C. Wang, C.Y. Chen, Functionalization of MWCNT by plasma treatment and use as additives for non-vacuum CuIn(S, Se)$_2$ nanoparticle deposition solar cells, J. Taiwan Inst. Chem. Eng., 80 (2017) 970–977.

[36] C. Zhang, F. Zhu, Z. Wang, L. Meng, Y. Liu, Amino functionalization of multiwalled carbon nanotubes by gamma ray irradiation and its epoxy composites, Polym. Compos., 33 (2012) 267–274.

[37] J.Y. Yook, J. Jun, S. Kwak, Amino functionalization of carbon nanotube surfaces with NH_3 plasa treatment, Appl. Surf. Sci., 256 (2010) 6941–6944.

[38] S. Mallakpour, A. Zadehnazari, Effect of amino acid-functionalized multi-walled carbon nanotubes on the properties of dopamine-based poly (amide-imide) composites: an experimental study, Bull. Mater. Sci., 37 (2014) 1065–1077.

[39] A. Stafiej, K. Pyrzynska, Adsorption of heavy metal ions with carbon nanotubes, Sep. Purif. Technol., 58 (2007) 49–52.

[40] B. Pan, D.H. Lin, H. Mashayekhi, B.S. Xing, Adsorption and hysteresis of bisphenol A and 17 alpha-ethinyl estradiol on carbon nanomaterials, Environ. Sci. Technol., 42 (2008) 5480–5485.

[41] L.L. Ji, W. Chen, L. Duan, D.Q. Zhu, Mechanisms for strong adsorption of tetracycline to carbon nanotubes: a comparative study using activated carbon and graphite as adsorbents, Environ. Sci. Technol., 43 (2009) 2322–2327.

[42] D.H. Lin, B.S. Xing, Adsorption of phenolic compounds by carbon nanotube: role of aromaticity and substitution of hydroxyl groups, Environ. Sci. Technol., 42 (2008) 7254–7259.

[43] Y. Yao, H. Bing, X. Feifei, C. Xiaofeng, Equilibrium and kinetic studies of methyl orange adsorption on multiwalled carbon nanotubes, Chem. Eng. J., 170 (2011) 82–89.

[44] S. Chatterjee, M.W. Lee, S.H. Woo, Adsorption of Congo red by chitosan hydrogel beads impregnated with carbon nanotubes, Bioresour. Technol., 101 (2010) 1800–1806.

[45] E. Bazrafshan, F.K. Mostafapour, A.R. Hosseini, A.K. Raksh, A.H. Mahvi, Decolorisation of reactive red 120 dye by using single-walled carbon nanotubes in aqueous solutions, J. Chem., 2013 (2013) 8 pages, http://dx.doi.org/10.1155/2013/938374.

[46] C.H. Wu, Adsorption of reactive dye onto carbon nanotubes: equilibrium, kinetics and thermodynamics, J. Hazard. Mater., 144 (2007) 93–100.

[47] H. Hyung, J.H. Kim, Natural organic matter (NOM) adsorption to multi-walled carbon nanotubes: effect of NOM characteristics and water quality parameters, Environ. Sci. Technol., 42 (2008) 4416–4421.

[48] C. Lu, Y.L. Chung, K-F. Chang, Adsorption of trihalomethanes from water with carbon nanotubes, Water Res., 39 (2005) 1183–1189.

[49] G.P. Rao, C. Lu, F. Su, Sorption of divalent metal ions from aqueous solution by carbon nanotubes: a review, Sep. Purif. Technol., 58 (2007) 224–231.

[50] Y.H. Li, J. Ding, Z.K. Luan, Z.C. Di, Y.F. Zhu, C.L. Xu, D.H. Wu, B.Q. Wei, Competitive adsorption of Pb^{2+}, Cu^{2+} and Cd^{2+} ions from aqueous solutions by multiwalled carbon nanotubes, Carbon, 41 (2003) 2787–2792.

[51] Y.H. Li, S. Wang, J. Wei, X. Zhang, C. Xu, Z. Luan, D. Wu, B. Wei, Lead adsorption on carbon nanotubes, Chem. Phys. Lett., 357 (2002) 263–266.

[52] K. Anitha, S. Namsani, J.K. Singh, Removal of heavy metal ions using a functionalized single-walled carbon nanotube: a molecular dynamics study, J. Phys. Chem. A, 119 (2015) 8349–8358.

[53] C. Lu, C. Liu, Removal of nickel(II) from aqueous solution by carbon nanotubes, J. Chem. Technol. Biotechnol., 81 (2006) 1932–1940.

[54] C. Lu, H. Chiu, Adsorption of zinc(II) from water with purified carbon nanotubes, Chem. Eng. Sci., 61 (2006) 1138–1145.

[55] V. Gupta, S. Agarwal, T.A. Saleh, Chromium removal by combining the magnetic properties of iron oxide with adsorption properties of carbon nanotubes, Water Res., 45 (2011) 2207–2212.

[56] Y.H. Li, Z.C. Di, J. Ding, D.H. Wu, Z.K. Luan, Y.Q. Zhu, Adsorption thermodynamic, kinetic and desorption studies of Pb^{2+} on carbon nanotubes, Water Res., 39 (2005) 605–609.

[57] C. Lu, H. Chiu, H. Bai, Comparisons of adsorbent cost for the removal of zinc (II) from aqueous solution by carbon nanotubes and activated carbon, J. Nanosci. Nanotechnol., 7 (2007) 1647–1652.

[58] D. Cohen-Tanugi, R.K. McGovern, S.H. Dave, J.H. Lienhard, J.C. Grossman, Quantifying the potential of ultra-permeable membranes for water desalination, Energy Environ. Sci., 7 (2014) 1134–1141.

[59] M. Bodzek, K. Konieczny, A. Kwiecińska-Mydlak, Nanotechnology in water and wastewater treatment. Graphene – the nanomaterial for manufacturing of next generation semipermeable membranes, Crit. Rev. Env. Sci. Technol., (2019) doi:10.1080/10643389.2019.1664258.

[60] X. Huang, X. Qi, F. Boey, H. Zhang, Graphene-based composites, Chem. Soc. Rev., 41 (2012) 666–686.

[61] B.M. Yoo, H.J. Shin, H.W. Yoon, H.B. Park, Graphene and graphene oxide and their uses in barrier polymers, J. Appl. Polym. Sci., 131 (2014) 39628.

[62] C. Santhosh, V. Velmurugan, G. Jacob, S.K. Jeong, A.N. Grace, A. Bhatnagar, Role of nanomaterials in water treatment applications: a review, Chem. Eng. J., 306 (2016) 1116–1137.

[63] R. Sitko, E. Turek, B. Zawisza, E. Malicka, E. Talik, J. Heimann, A. Gagor, B. Feist, R. Wrzalik, Adsorption of divalent metal ions from aqueous solutions using graphene oxide, Dalton Trans., 42 (2013) 5682–5689.

[64] H. Wang, X.Z. Yuan, Y. Wu, H.J. Huang, G.M. Zeng, Y. Liu, X.L. Wang, N.B. Lin, Y. Qi, Adsorption characteristics and behaviors of graphene oxide for Zn(II) removal from aqueous solution, Appl. Surf. Sci., 279 (2013) 432–440.

[65] C.J. Madadrang, H.Y. Kim, G.H. Gao, N. Wang, J. Zhu, H. Feng, M. Gorring, M.L. Kasner, S.F. Hou, Adsorption behavior of EDTA-graphene oxide for Pb (II) removal, ACS Appl. Mater. Interfaces, 4 (2012) 1186–1193.

[66] Z.-H. Huang, X. Zheng, W. Lv, M. Wang, Q.-H. Yang, F. Kang, Adsorption of lead(II) ions from aqueous solution on low-temperature exfoliated graphene nanosheets, Langmuir, 27 (2011) 7558–7562.

[67] S. Kumar, R.R. Nair, P.B. Pillai, S.N. Gupta, M.A.R. Iyengar, A.K. Sood, Graphene oxide–MnFe$_2$O$_4$ magnetic nanohybrids for efficient removal of lead and arsenic from water, ACS Appl. Mater. Interfaces, 6 (2014) 17426–17436.

[68] Y.-C, Lee, J.-W, Yang, Self-assembled flower-like TiO$_2$ on exfoliated graphite oxide for heavy metal removal, J. Ind. Eng. Chem., 18 (2012) 1178–1185.

[69] L. Xu, J. Wang, The application of graphene-based materials for the removal of heavy metals and radionuclides from water and wastewater, Crit. Rev. Env. Sci. Technol., 47 (2017) 1042–1105.

[70] J. Li, S. Zhang, C. Chen, G. Zhao, X. Yang, J. Li, X. Wang, Removal of Cu(II) and fulvic acid by graphene oxide nanosheets decorated with Fe$_3$O$_4$ nanoparticles, ACS Appl. Mater. Interfaces, 4 (2012) 4991–5000.

[71] J. Hur, J. Shin, J. Yoo, Y.-S. Seo, Competitive adsorption of metals onto magnetic graphene oxide: comparison with other carbonaceous adsorbents, Sci. World J., 2015 (2015) 11 pages, https://doi.org/10.1155/2015/836287.

[72] D. Nandi, T. Basu, S. Debnath, A.K. Ghosh, A. De, U.C. Ghosh, Mechanistic insight for the sorption of Cd(II) and Cu(II) from aqueous solution on magnetic mn-doped Fe(III) oxide nanoparticle implanted graphene, J. Chem. Eng. Data, 58 (2013) 2809–2818.

[73] Y. Wang, S. Liang, B. Chen, F. Guo, S. Yu, Y. Tang, Synergistic removal of Pb(II), Cd(II) and humic acid by Fe$_3$O$_4$@mesoporous silica–graphene oxide composites, PLoS One, 8 (2013) e65634.

[74] L. Hao, H. Song, L. Zhang, X. Wan, Y. Tang, Y. Lv, SiO$_2$/graphene composite for highly selective adsorption of Pb(II) ion, J. Colloid Interface Sci., 369 (2012) 381–387.

[75] S.P.Lee, G.A.M. Ali, H. Algarni, K.F. Chong, Flake size-dependent adsorption of graphene oxide aerogel, J. Mol. Liq., 277 (2019) 175–180.

[76] X. Li, J.J. Lenhart, H.W. Walker, Aggregation kinetics and dissolution of coated silver nanoparticles, Langmuir, 28 (2011) 1095–1104.

[77] S. Vasudevan, J. Lakshmi, The adsorption of phosphate by graphene from aqueous solution, RSC Adv., 2 (2012) 5234–5242.

[78] S. Zhang, Y. Shao, J. Liu, I.A. Aksay, Y. Lin, Graphene-polypyrrole nanocomposite as a highly efficient and low cost electrically switched ion exchange for removing ClO$_4^-$ from wastewater, ACS Appl. Mater. Interfaces, 3 (2011) 3633–3637.

[79] T. Hartono, S. Wang, Q. Ma, Z. Zhu, Layer structured graphite oxide as a novel adsorbent for humic acid removal from aqueous solution, J. Colloid Interface Sci., 333 (2009) 114–119.

[80] Y. Gao, Y. Li, L. Zhang, H. Huang, J. Hu, S.M. Shah, X. Su, Adsorption and removal of tetracycline antibiotics from aqueous solution by graphene oxide, J. Colloid Interface Sci., 368 (2012) 540–546.

[81] F. Liu, S. Chung, G. Oh, T.S. Seo, Three-dimensional graphene oxide nanostructure for fast and efficient water-soluble dye removal, ACS Appl. Mater. Interfaces, 4 (2012) 922–927.

[82] L. Ai, J. Jiang, Removal of methylene blue from aqueous solution with self-assembled cylindrical graphene–carbon nanotube hybrid, Chem. Eng. J., 192 (2012) 156–163.

[83] X. Zhang, C. Cheng, J. Zhao, L. Ma, S. Sun, C. Zhao, Polyethersulfone enwrapped graphene oxide porous particles for water treatment, Chem. Eng. J., 215 (2013) 72–81.

[84] G. Xie, P. Xi, H. Liu, F. Chen, L. Huang, Y. Shi, F. Hou, Z. Zeng, C. Shao, J. Wang, A facile chemical method to produce superparamagnetic graphene oxide–Fe$_3$O$_4$ hybrid composite and its application in the removal of dyes from aqueous solution, J. Mater. Chem., 22 (2012) 1033–1039.

[85] X. Wang, H. Tian, Y. Yang, H. Wang, S. Wang, W. Zheng, Y. Liu, Reduced graphene oxide/CdS for efficiently photocatalystic degradation of methylene blue, J. Alloys Compd., 524 (2012) 5–12.

[86] S. Bai, X. Shen, X. Zhong, Y. Liu, G. Zhu, X. Xu, K. Chen, One-pot solvothermal preparation of magnetic reduced graphene oxideferrite hybrids for organic dye removal, Carbon, 50 (2012) 2337–2346.

[87] P. Bradder, S.K. Ling, S. Wang, S. Liu, Dye adsorption on layered graphite oxide, J. Chem. Eng. Data, 56 (2010) 138–141.

[88] M. Rajabi, K. Mahanpoor, O. Moradi, Removal of dye molecules from aqueous solution by carbon nanotubes and carbon nanotube functional groups: critical review, RSC Adv., 7 (2017) 47083–47090.

[89] X. Shi, W. Ruan, J. Hu, M. Fan, R. Cao, X. Wei, Optimizing the removal of rhodamine B in aqueous solutions by reduced graphene oxide-supported nanoscale zerovalent iron (NZVI/RGO) using an artificial neural network-genetic algorithm (ANN-GA), Nanomaterials, 7 (2017) 134.

[90] S.M.S. Arabi, R.S. Lalehloo, M.R.T.B. Olyai, G.A.M. Ali, H. Sadegh, Removal of Congo Red azo dye from aqueous solution by ZnO nanoparticles loaded on multiwall carbon nanotubes, Physica E., 106 (2019) 150–155.

[91] V.K. Gupta, S. Agarwal, H. Sadegh, G.A.M. Ali, A.K. Bharti, A.S.H. Makhlouf, Facile route synthesis of novel graphene oxide-β-cyclodextrin nanocomposite and its application as adsorbent for removal of toxic bisphenol A from the aqueous phase, J. Mol. Liq., 237 (2017) 466–472.

[92] J. Ma, M. Yang, F. Yu, J. Zheng, Water-enhanced removal of ciprofloxacin from water by porous graphene hydrogel, Sci. Rep., 5 (2015) 13578.

[93] F. Yu, J. Ma, D. Bi, Enhanced adsorptive removal of selected pharmaceutical antibiotics from aqueous solution by activated graphene, Environ. Sci. Pollut. Res. Int., 22 (2015) 4715–4724.

[94] H. Chen, B. Gao, H. Li, Removal of sulfamethoxazole and ciprofloxacin from aqueous solutions by graphene oxide, J. Hazard. Mater., 282 (2015) 201–207.

[95] L. Zhao, F. Xue, B. Yu, J. Xie, X. Zhang, R. Wu, R. Wang, Z. Hu, S.-T. Yang, J. Luo, TiO$_2$–graphene sponge for the removal of tetracycline, J. Nanopart. Res., 17 (2015) 16.

[96] E.E. Ghadim, F. Manouchehri, G. Soleimani, H. Hosseini, S. Kimiagar, S. Nafisi, Adsorption properties of tetracycline onto graphene oxide: equilibrium, kinetic and thermodynamic studies, PLoS One, 8 (2013) e79254.

[97] Y. Lin, S. Xu, J. Li, Fast and highly efficient tetracyclines removal from environmental waters by graphene oxide functionalized magnetic particles, Chem. Eng. J., 225 (2013) 679–685.

[98] A. Kassem, G.M. Ayoub, L.Malaeb, Antibacterial activity of chitosan nano-composites and carbon nanotubes: a review, Sci. Total Environ., 668 (2019) 566–576.

[99] J. Fabrega, S.N. Luoma, C.R. Tyler, T.S. Galloway, J.R. Lead, Silver nanoparticles: behaviour and effects in the aquatic environment, Environ. Int., 37 (2011) 517–531.

[100] M.C. Daniel, D. Astruc, Gold nanoparticles: assembly, supramolecular chemistry, quantum-size-related properties, and applications toward biology, catalysis, and nanotechnology, Chem. Rev., 104 (2004) 293–346.

[101] L. Feng, M. Cao, X. Ma, Y. Zhu, C. Hu, Superparamagnetic high-surface- area Fe_3O_4 nanoparticles as adsorbents for arsenic removal, J. Hazard. Mater., 217–218 (2012) 439–446.

[102] K. Gupta, S. Bhattacharya, D. Chattopadhyay, A. Mukho-padhyay, H. Biswas, J. Dutta, N.R. Ray, U.C. Ghosh, Ceria associated manganese oxide nanoparticles: synthesis, characterization and arsenic(V) sorption behavior, Chem. Eng. J., 172 (2011) 219–229.

[103] T. Luo, J. Cui, S. Hu, Y. Huang, C. Jing, Arsenic removal and recovery from copper smelting wastewater using TiO_2, Environ. Sci. Technol., 44 (2010) 9094–9098.

[104] C. Gao, W. Zhang, H. Li, L. Lang, Z. Xu, Controllable fabrication of mesoporous MgO with various morphologies and their absorption performance for toxic pollutants in water, Cryst. Growth Des., 8 (2008) 3785–3790.

[105] A. Goswamia, P.K. Raul, M.K. Purkait, Arsenic adsorption using copper (II) oxide nanoparticles, Chem. Eng. Res. Des., 90 (2012) 1387–1396.

[106] C.Y. Cao, Z.M. Cui, C.Q. Chen, W.G. Song, W. Cai, Ceria hollow nanospheres produced by a template-free microwave-assisted hydrothermal method for heavy metal ion removal and catalysis, J. Phys. Chem. C, 114 (2010) 9865–9870.

[107] M. Hua, S. Zhang, B. Pan, W. Zhang, L. Lv, Q. Zhang, Heavy metal removal from water/wastewater by nanosized metal oxides: a review, J. Hazard. Mater., 211–212 (2012) 317–331.

[108] P. Lakshmipathiraj, B. Narasimhan, S. Prabhakar, G.B. Raju, Adsorption of arsenate on synthetic goethite from aqueous solutions, J. Hazard. Mater., 136 (2006) 281–287.

[109] K.E. Engates, H.J. Shipley, Adsorption of Pb, Cd, Cu, Zn, and Ni to titanium dioxide nanoparticles: effect of particle size, solid concentration, and exhaustion, Environ. Sci. Pollut. Res. Int., 18 (2011) 386–395.

[110] R.-F. Yu, F.-H. Chi, W.-P. Cheng, J.-C. Chang, Application of pH, ORP, and DO monitoring to evaluate chromium(VI) removal from wastewater by the nanoscale zerovalent iron (nZVI) process, Chem. Eng. J., 255 (2014) 568–576.

[111] Z. Wen, Y. Zhang, C. Dai, Removal of phosphate from aqueous solution using nanoscale zerovalent iron (nZVI), Colloids Surf., A, 457 (2014) 433–440.

[112] J. Fan, G. Yuo, J. Wang, M. Fan, Rapid decolorization of azo dye methyl orange in aqueous solution by nanoscale zerovalent iron particles, J. Hazard. Mater., 166 (2009) 904–910.

[113] I. Gehrke, A. Geiser, A. Somborn-Schulz, Innovations in nanotechnology for water treatment, Nanotechnol. Sci. Appl., 8 (2015) 1–17.

[114] M.H. Mashhadizadeh, M. Amoli-Diva, Atomic absorption spectrometric determination of Al^{3+} and Cr^{3+} after preconcen-tration and separation on 3-mercaptopropionic acid modified silica coated-Fe_3O_4 nanoparticles, J. Anal. At. Spectrom., 28 (2013) 251–258.

[115] M.A. Karimi, A. Hatefi-Mehrjardi, S.Z. Mohammadi, A. Mohadesi, M. Mazloum-Ardakani, A.A. Kabir, M. Kazemi-pour, N. Afsahi, Solid phase extraction of trace amounts of silver (I) using dithizone-immobilized alumina-coated magnetite nanoparticles prior to determination by flame atomic absorption spectrometry, Int. J. Environ. Anal. Chem., 92 (2012) 1325–1340.

[116] Q. Li, M.H.W. Lam, R.S.S. Wu, B. Jiang, Rapid magnetic-mediated solid-phase extraction and pre-concentration of selected endocrine disrupting chemicals in natural waters by poly(divinylbenzene-co-methacrylic acid) coated Fe_3O_4 core-shell magnetite microspheres for their liquid chromatography-tandem mass spectrometry determination, J. Chromatogr. A, 1217 (2010) 1219–1226.

[117] N. Pandey, S.K. Shukla, N.B. Singh, Water purification by polymer nanocomposites: an overview, Nanocomposites, 3 (2017) 47–66.

[118] M. Runowski, Nanotechnology – nanomaterials, nanoparticles and multifunctional nanostructures core/coating type, Chemik, 68 (2014) 766–775 (in Polish).

[119] T. Tosco, P.M. Papini, C.C. Viggi, R. Sethi, Nanoscale zerovalent iron particles for groundwater remediation: a review, J. Cleaner Prod., 77 (2014) 10–21.

[120] P. Xu, G.M. Zeng, D.L. Huang, C.L. Feng, S. Hu, M.H. Zhao, C. Lai, Z. Wei, C. Huang, G.X. Xie, Z.F. Liu, Use of iron oxide nanomaterials in wastewater treatment: a review, Sci. Total Environ., 424 (2012) 1–10.

[121] S. Dubey, S. Banerjee, S.N. Upadhyay, Y.C. Sharma, Application of common nano-materials for removal of selected metallic species from water and wastewaters: a critical review, J. Mol. Liq., 240 (2017) 656–677.

[122] R.A. Crane, M. Dickinson, I.C. Popescu, T.B. Scott, Magnetite and zero-valent iron nanoparticles for the remediation of uranium contaminated environmental water, Water Res., 45 (2011) 2931–2942.

[123] S.L. Li, W. Wang, W.L. Yan, W.X. Zhang, Nanoscale zero-valent iron (nZVI) for the treatment of concentrated Cu(II) wastewater: a field demonstration, Environ. Sci. Processes Impacts, 16 (2014) 524–533.

[124] M.A.V. Ramos, W. Yan, X.Q. Li, B.E. Koel, W.X. Zhang, Simultaneous oxidation and reduction of arsenic by zero-valent iron nanoparticles: understanding the significance of the core-shell structure, J. Phys. Chem. C, 113 (2009) 14591–14594.

[125] A. Ryu, S.-W. Jeong, A. Jang, H. Choi, Reduction of highly concentrated nitrate using nanoscale zero-valent iron: effects of aggregation and catalyst on reactivity, Appl. Catal., B, 105 (2011) 128–135.

[126] Z. Fang, J. Chen, X. Qiu, X. Qiu, W. Cheng, L. Zhu, Effective removal of antibiotic metronidazole from water by nanoscale zero-valent iron particles, Desalination, 268 (2011) 60–67.

[127] N. Chauhan, S. Gupta, N. Singh, S. Singh, S.S. Islam, K.N. Sood, R. Pasricha, Aligned nanogold assisted one step sensing and removal of heavy metal ions, J. Colloid Interface Sci., 363 (2011) 42–50.

[128] Y.F. Lee, F.H. Nan, M.J. Chen, H.Y. Wu, C.W. Ho, Y.Y. Chen, C.C. Huang, Detection and removal of mercury and lead ions by using gold nanoparticle-based gel membrane, Anal. Methods, 4 (2012) 1709–1717.

[129] B. Nowack, H.F. Krug, M. Height, 120 y of nanosilver history: implications for policy makers, Environ. Sci. Technol., 45 (2011) 1177–1183.

[130] C. Zhang, Z. Hu, B. Deng, Silver nanoparticles in aquatic environments: physiochemical behavior and antimicrobial mechanisms, Water Res., 88 (2016) 403–427.

[131] R.S. Kalhapure, S.J. Sonawane, D.R. Sikwal, M. Jadhav, S. Rambharose, C. Mocktar, T. Govender, Solid lipid nano-particles of clotrimazole silver complex: an efficient nano antibacterial against Staphylococcus aureus and MRSA, Colloids Surf., B, 136 (2015) 651–658.

[132] B. Borrego, G. Lorenzo, J.D. Mota-Morales, H. Almanza-Reyes, F. Mateos, E. López-Gil, N. de la Losa, V.A. Burmistrov, A.N. Pestryakov, A. Brun, Potential application of silver nanoparticles to control the infectivity of Rift Valley fever virus in vitro and in vivo, Nanomed. Nanotechnol. Biol. Med., 12 (2016) 1185–1192.

[133] I. Sondi, B. Salopek-Sondi, Silver nanoparticles as anti-microbial agent: a case study on E. coli as a model for Gram-negative bacteria, J. Colloid Interface Sci., 275 (2004) 177–182.

[134] D.V. Quang, P.B. Sarawade, S.J. Jeon, S.H. Kim, J.-K. Kim, Y.G. Chai, H.T. Kim, Effective water disinfection using silver nanoparticle containing silica beads, Appl. Surf. Sci., 266 (2013) 280–287.

[135] V. Bokare, J.-L. Jung, Y.-Y. Chang, Y.-S. Chang, Reductive dechlorination of octachlorodibenzo-p-dioxin by nanosized zerovalent zinc: modelling of rate kinetics and congener profile, J. Hazard. Mater., 250 (2013) 397–402.

[136] P.G. Tratnyek, A.J. Salter, J.T. Nurmi, V. Sarathy, Environmental Applications of Zerovalent Metals: Iron vs. Zinc, In: Nanoscale Materials in Chemistry: Environmental Applications, ACS Publications, Washington D.C., USA, 2010, pp. 165–178.

[137] P. Trivedi, L. Axe, Modeling Cd and Zn sorption to hydrous metal oxides, Environ. Sci. Technol., 34 (2000) 2215–2223.

[138] S. Yean, L. Cong, C.T. Yavuz, J.T. Mayo, W.W. Yu, A.T. Kan, V.L. Colvin, M.B. Tomson, Effect of magnetite particle size on

adsorption and desorption of arsenite and arsenate, J. Mater. Res., 20 (2005) 3255–3264.

[139] Y.C. Sharma, V. Srivastava, V.K. Singh, S.N. Kaul, C.H.Weng, Nano-adsorbents for the removal of metallic pollutants from water and wastewater, Environ. Technol., 30 (2009) 583–609.

[140] K.D. Hristovski, H. Nguyen, P.K. Westerhoff, Removal of arsenate and 17-ethinyl estradiol (EE2) by iron (hydr)oxide modified activated carbon fibers, J. Environ. Sci. Health. Part A Toxic/Hazard. Subst. Environ. Eng., 44 (2009) 354–361.

[141] J. Hu, G.H. Chen, I.M.C. Lo, Selective removal of heavy metals from industrial wastewater using maghemite nanoparticle: performance and mechanisms, J. Environ. Eng.-ASCE, 132 (2006) 709–715.

[142] M. Mohapatra, K. Rout, S.K. Gupta, P. Singh, S. Anand, B.K. Mishra, Facile synthesis of additive-assisted nano goethite powder and its application for fluoride remediation, J. Nanopart. Res., 12 (2009) 681–686.

[143] Y.H. Chen, F.A. Li, Kinetic study on removal of copper(II) using goethite and hematite nano-photocatalysts, J. Colloid Interface Sci., 347 (2010) 277–281.

[144] H.J. Shipley, K.E. Engates, V.A. Grover, Removal of Pb(II), Cd(II), Cu(II), and Zn(II) by hematite nanoparticles: effect of sorbent concentration, pH, temperature, and exhaustion, Environ. Sci. Pollut. Res. Int., 20 (2013) 1727–1736.

[145] J. Hu, I. Lo, G. Chen, Removal of Cr (VI) by magnetite, Water Sci. Technol., 50 (2004) 139–146.

[146] S.-Y. Mak, D.-H. Chen, Fast adsorption of methylene blue on polyacrylic acid-bound iron oxide magnetic nanoparticles, Dyes Pigm., 61 (2004) 93–98.

[147] R. Akhbarizadeh, M.R. Shayesterfar, E. Darezereshki, Competitive removal of metals from wastewater by maghemite nanoparticles: a comparison between simulated wastewater and AMD, Mine Water Environ., 33 (2014) 89–96.

[148] K.L. Mercer, J.E. Tobiason, Removal of arsenic from high ionic strength solutions: effects of ionic strength, pH, and preformed vs. in situ formed HFO, Environ. Sci. Technol., 42 (2008) 3797–3802.

[149] S.A. Klein, B.M. Pawlik, The removal of arsenic from water using natural iron oxide minerals, J. Cleaner Prod., 29–30 (2012) 208–213.

[150] F. Ge, M.-M. Li, H. Ye, B.-X. Zhao, Effective removal of heavy metal ions Cd^{2+}, Zn^{2+}, Pb^{2+}, Cu^{2+} from aqueous solution by polymer-modified magnetic nanoparticles, J. Hazard. Mater., 211 (2012) 366–372.

[151] M. Palimi, M. Rostami, M. Mahdavian, B. Ramezanzadeh, Surface modification of Fe_2O_3 nanoparticles with 3-aminopropyltrimethoxysilane (APTMS): an attempt to investigate surface treatment on surface chemistry and mechanical properties of polyurethane/Fe_2O_3 nanocomposites, Appl. Surf. Sci., 320 (2014) 60–72.

[152] I. Tyagi, V. Gupta, H. Sadegh, R. Ghoshekandi, A.S.H. Makhlouf, Nanoparticles as adsorbent; a positive approach for removal of noxious metal ions: a review, Sci. Technol. Dev., 34 (2017) 95–214.

[153] R.A. Khaydarov, R.R. Khaydarov, O. Gapurova, Water purification from metal ions using carbon nanoparticle-conjugated polymer nanocomposites, Water Res., 44 (2010) 1927–1933.

[154] Y. Pang, G. Zeng, L. Tang, Y. Zhang, Y. Liu, X. Lei, Z. Li, J. Zhang, G. Xie, PEI grafted magnetic porous powder for highly effective adsorption of heavy metal ions, Desalination, 281 (2011) 278–284.

[155] L. Cumbal, A.K. Sengupta, Arsenic removal using polymer-supported hydrated iron(III) oxide nanoparticles: role of donnan membrane effect, Environ. Sci. Technol., 39 (2005) 6508–6515.

[156] K. Zargoosh, H. Abedini, A. Abdolmaleki, M.R. Molavian, Effective removal of heavy metal ions from industrial wastes using thiosalicylhydrazide-modified magnetic nanoparticles, Ind. Eng. Chem. Res., 52 (2013) 14944–14954.

[157] L. Zhi, J. Liu, Y. Wang, W. Zhang, B. Wang, Z. Xu, Z. Yang, X. Huo, G. Li, Multifunctional Fe_3O_4 nanoparticles for highly

[158] L. Zhang, T. Huang, M. Zhang, X. Guo, Z. Yuan, Studies on the capability and behavior of adsorption of thallium on nano-Al_2O_3, J. Hazard. Mater., 157 (2008) 352–357.

[159] A. Afkhami, M. Saber-Tehrani, H. Bagheri, Simultaneous removal of heavy-metal ions in wastewater samples using nano-alumina modified with 2,4-dinitrophenylhydrazine, J. Hazard. Mater., 181 (2010) 836–844.

[160] S.S. Tripathy, J.L. Bersillon, K. Gopal, Adsorption of Cd^{2+} on hydrous manganese dioxide from aqueous solutions, Desalination, 194 (2006) 11–21.

[161] S.P. Mishra, S.S. Dubey, D. Tiwari, Inorganic particulates in removal of heavy metal toxic ions: IX. Rapid and efficient removal of Hg (II) by hydrous manganese and tin oxides, J. Colloid Interface Sci., 279 (2004) 61–67.

[162] H. Choi, E. Stathatos, D.D. Dionysiou, Sol-gel preparation of mesoporous photocatalytic TiO_2 films and TiO_2/Al_2O_3 composite membranes for environmental applications, Appl. Catal., B., 63 (2006) 60–67.

[163] S. Anandan, K. Kathiravan, V. Murugesan, Y. Ikuma, Anionic (IO_3^{3-}) non-metal doped TiO_2 nanoparticles for the photocatalytic degradation of hazardous pollutant in water, Catal. Commun., 10 (2009) 1014–1019.

[164] A.D. Mani, P.M.K. Reddy, M. Srinivaas, P. Ghosal, N. Xanthopoulos, C. Subrahmanyam, Facile synthesis of efficient visible active C-doped TiO_2 nanomaterials with high surface area for the simultaneous removal of phenol and Cr(VI), Mater. Res. Bull., 61 (2015) 391–399.

[165] R. George, N. Bahadur, N. Singh, R. Singh, A. Verma, A.K. Shukla, Environmentally benign TiO_2 nanomaterials for removal of heavy metal ions with interfering ions present in tap water, Mater. Today:. Proc., 3 (2016) 162–166.

[166] W. Liu, W. Sun, Y. Han, M. Ahmadb, J. Ni, Adsorption of Cu(II) and Cd(II) on titanate nanomaterials synthesized via hydrothermal method under different NaOH concentrations: role of sodium content, Colloids Surf., A, 452 (2014) 138–147.

[167] Y. Chang, W. Han, A. Cai, H. Wang, Synthesis of lignosulfonate-assisted flower-like titanate nanostructures and their excellent performance for heavy metal removal, Ceram. Int., 42 (2016) 8645–8649.

[168] H.Z. Zhang, J.F. Banfield, Understanding polymorphic phase transformation behavior during growth of nanocrystalline aggregates: insights from TiO_2, J. Phys. Chem. B, 104 (2000) 3481–3487.

[169] J. Lonnen, S. Kilvington, S.C. Kehoe, F. Al-Touati, K.G. McGuigan, Solar and photocatalytic disinfection of protozoan, fungal and bacterial microbes in drinking water, Water Res., 39 (2005) 877–883.

[170] R. Fagan, D.E. McCormack, D.D. Dionysiou, S.C. Pillai, A review of solar and visible light active TiO_2 photocatalysis for treating bacteria, cyanotoxins and contaminants of emerging concern, Mater. Sci. Semicond. Process., 42 (2016) 2–14.

[171] S. Gelover, P. Mondragón, A. Jiménez, Titanium dioxide sol–gel deposited over glass and its application as a photocatalyst for water decontamination, J. Photochem. Photobiol., A, 165 (2004) 241–246.

[172] M.A. Rahman, M. Mohd, Photocatalysed degradation of two selected pesticide derivatives, dichlorvos and phosphamidon, in aqueous suspensions of titanium dioxide, Desalination, 181 (2005) 161–172

[173] M. Flytzani-Stephanopoulos, M. Sakbodin, Z. Wang, Regenerative adsorption and removal of H_2S from hot fuel gas streams by rare earth oxides, Science, 312 (2006) 1508–1510.

[174] X. Wang, W. Cai, Y. Lin, G. Wang, C. Liang, Mass production of micro/nanostructured porous ZnO plates and their strong structurally enhanced and selective adsorption performance for environmental remediation, J. Mater. Chem., 20 (2010) 8582–8590.

[175] T. Sheela, Y.A. Nayaka, R. Viswanatha, S. Basavanna, T.G. Venkatesha, Kinetics and thermodynamics studies on the adsorption of Zn(II), Cd(II) and Hg(II) from aqueous

solution using zinc oxide nanoparticles, Powder Technol., 217 (2012) 163–170.

[176] C. Gomez-Solís, J. Ballesteros, L. Torres-Martínez, I. Juárez-Ramírez, L.D. Torres, M.E. Zarazua-Morin, S.W. Lee, Rapid synthesis of ZnO nano-corncobs from Nital solution and its application in the photodegradation of methyl orange, J. Photochem. Photobiol., A, 298 (2015) 49–54.

[177] K.M. Lee, C.W. Lai, K.S. Ngai, J.C. Juan, Recent developments of zinc oxide based photocatalyst in water treatment technology: a review, Water Res., 88 (2016) 428–448.

[178] K. Dai, L. Lu, C. Liang, J. Dai, G. Zhu, Z. Liu, Q. Liu, Y. Zhang, Graphene oxide modified ZnO nanorods hybrid with high reusable photocatalytic activity under UV-LED irradiation, Mater. Chem. Phys., 143 (2014) 1410–1416.

[179] M.T. Uddin, Y. Nicolas, C.L. Olivier, T. Toupance, L. Servant, M.M. Müller, H.-J. Kleebe, J. Ziegler, W. Jaegermann, Nano-structured SnO_2–ZnO heterojunction photocatalysts showing enhanced photocatalytic activity for the degradation of organic dyes, Inorg. Chem., 51 (2012) 7764–7773.

[180] M. Samadi, A. Pourjavadi, A. Moshfegh, Role of CdO addition on the growth and photocatalytic activity of electrospun ZnO nanofibers: UV vs. visible light, Appl. Surf. Sci., 298 (2014)147–154.

[181] H.R. Pant, C.H. Park, B. Pant, L.D. Tijing, H.Y. Kim, C.S. Kim, Synthesis, characterization, and photocatalytic properties of ZnO nano-flower containing TiO_2 NPs, Ceram. Int., 38 (2012) 2943–2950.

[182] P.R. Grossl, D.L. Sparks, C.C. Ainsworth, Rapid kinetics of Cu (II) adsorption/desorptionon goethite, Environ. Sci. Technol., 28 (1994) 1422–1429.

[183] X. Wei, S. Bhojappa, L.S. Lin, R.C. Viadero, Performance of Nano-magnetite for removal of selenium from aqueous solutions, Environ. Eng. Sci., 29 (2012) 526–532.

[184] A.A. Babaei, Z. Baboli, N. Jaafarzadeh, G. Goudarzi, M. Bahrami, M. Ahmadi, Synthesis, performance, and non-linear modeling of modified nano-sized magnetite for removal of Cr (VI) from aqueous solutions, Desal. Water Treat., 53 (2015) 768–777.

[185] Y. Liu, M. Chen, Y. Hao, Study on the adsorption of Cu (II) by EDTA functionalized Fe_3O_4 magnetic nano particles, Chem. Eng. J., 218 (2013) 46–54.

[186] J. Zhang, S. Zhai, S. Li, Z. Xiao, Y. Song, Q. An, G. Tian, Pb (II) removal of Fe_3O_4@SiO_2–NH_2 core – shell nanomaterials prepared via a controllable sol – gel process, Chem. Eng. J., 215–216 (2013) 461–471.

[187] H. Karami, Heavy metal removal from water by magnetite nanorods, Chem. Eng. J., 219 (2013) 209–216.

[188] T. Nur, P. Loganathan, T.C. Nguyen, S. Vigneswaran, G. Singh, J. Kandasamy, Batch and column adsorption and desorption of fluoride using hydrous ferric oxide: solution chemistry and modeling, Chem. Eng. J., 247 (2014) 93–102.

[189] Y.C. Sharma, V. Srivastava, A.K. Mukherjee, Synthesis and application of nano-Al_2O_3 powder for the reclamation of hexavalent chromium from aqueous solutions, J. Chem. Eng. Data, 55 (2010) 2390–2398.

[190] V. Srivastava, C.H. Weng, V.K. Singh, Y.C. Sharma, Adsorption of nickel ions from aqueous solutions by nano alumina: kinetic, mass transfer, and equilibrium studies, J. Chem. Eng. Data, 56 (2011) 1414–1422.

[191] A. Rahmani, H.Z. Mousavi, M. Fazli, Effect of nanostructure alumina on adsorption of heavy metals, Desalination, 253 (2010) 94–100.

[192] A.M. Mahmoud, F.A. Ibrahim, S.A. Shaban, N.A. Youssef, Adsorption of heavy metal ion from aqueous solution by nickel oxide nano catalyst prepared by different methods, Egypt. J. Pet., 24 (2015) 27–35.

[193] J. Mukherjee, J. Ramkumar, S. Chandramouleeswaran, R. Shukla, A.K. Tyagi, Sorption characteristics of nano manganese oxide: efficient sorbent for removal of metal ions from aqueous streams, J. Radioanal. Nucl. Chem., 297 (2013) 49–57.

[194] H. Zhan, Y. Jiang, Q. Ma, Determination of adsorption characteristics of metal oxide nanomaterials: application as adsorbents, Anal. Lett., 47 (2014) 871–884.

[195] V.K. Gupta, R. Chandra, I. Tyagi, M. Verma, Removal of hexavalent chromium ions using CuO nanoparticles for water purification applications, J. Colloid Interface Sci., 478 (2016) 54–62.

[196] X. Zhang, J. Liu, S.J. Kell, X. Huang, J. Liu, Biomimetic snowflakeshaped magnetic micro-/nanostructures for highly efficient adsorption of heavy metal ions and organic pollutants from aqueous solution, J. Mater. Chem. A, 2 (2014) 11759–11767.

[197] Y. Tu, C. You, C. Chang, Kinetics and thermodynamics of adsorption for Cd on green manufactured nano-particles, J. Hazard. Mater., 235–236 (2012) 116–122.

[198] J. Jordan, K.I. Jacob, R. Tannenbaum, M.A. Sharaf, I. Jasiuk, Experimental trends in polymer nanocomposites – a review, Mater. Sci. Eng., A, 393 (2005) 1–11.

[199] X. Zhao, L. Lv, B.C. Pan, W.M. Zhang, S.J. Zhang, Q.X. Zhang, Polymer-supported nanocomposites for environmental application: a review, Chem. Eng. J., 170 (2011) 381–394.

[200] G. Lofrano, M. Carotenuto, G. Libralato, R.F. Domingos, A. Markus, L. Dini, R.K. Gautam, D. Baldantoni, M. Rossi, S.K. Sharma, M.C. Chattopadhyaya, M. Giugni, S. Meric, Polymer functionalized nanocomposites for metals removal from water and wastewater: an overview, Water Res., 92 (2016) 22–37.

[201] C.S.C. Chiew, H.K. Yeoh, P. Pasbakhsh, K. Krishnaiah, P.E. Poh, B.T. Tey, E.S. Chan, Halloysite/algina H.K.te nanocomposite beads: kinetics, equilibrium and mechanism for lead adsorption, Appl. Clay Sci., 119 (2016) 301–310.

[202] U.Baig, R.A.K. Rao, A.A. Khan, M.M. Sanagi, M.A. Gondal, Removal of carcinogenic hexavalent chromium from aqueous solutions using newly synthesized and characterized poly-pyrrole-titanium(IV)phosphate nanocornposite, Chem. Eng. J., 280 (2015) 494–504.

[203] R.Bushra, M.Naushad, R. Adnan, Z.A. Alothman, M. Rafatullah, Polyaniline supported nanocomposite cation exchanger: synthesis, characterization and applications for the efficient removal of Pb^{2+} ion from aqueous medium, J. Ind. Eng. Chem., 21 (2015) 1112–1118.

[204] L. Chen, X. Zhao, B.C. Pan, W.X. Zhang, M. Hua, L. Lv, W.M. Zhang, Preferable removal of phosphate from water using hydrous zirconium oxide-based nanocomposite of high stability, J. Hazard. Mater., 284 (2015) 35–42.

[205] Q.R. Zhang, Q. Du, M. Hua, T.F. Jiao, G.F. Mao, B.C. Pan, Sorption enhancement of lead ions from water by surface charged polystyrene-supported nano-zirconium oxide composites, Environ. Sci. Technol., 47 (2013) 6536–6544.

[206] D. Wang, A critical review of cellulose-based nanomaterials for water purification in industrial processes, Cellulose, 26 (2019) 687–701.

[207] E. Vunain, A.K. Mishra, B.B. Mamba, Dendrimers, mesoporous silicas and chitosanbased nanosorbents for the removal of heavy-metal ions: a review, Int. J. Biol. Macromol., 86 (2016) 570–586.

[208] K.Y. Foo, B.H. Hameed, Decontamination of textile waste-water via TiO2/activated carbon composite materials, Adv. Colloid Interface Sci., 159 (2010) 130–143.

[209] J.A. Arcibar-Orozco, M. Avalos-Borja, J.R. Rangel-Mendez, Effect of phosphate on the particle size of ferric oxyhydroxides anchored onto activated carbon: As(V) removal from water, Environ. Sci. Technol., 46 (2012) 9577–9583.

[210] Y. Kikuchi, Q. Qian, M. Machida, H. Tatsumoto, Effect of ZnO loading to activated carbon on Pb(II) adsorption from aqueous solution, Carbon, 44 (2006) 195–202.

[211] P.Y. Furlan, M.E. Melcer, Removal of aromatic pollutant surrogate from water by recyclable magnetite-activated carbon nanocomposite: an experiment for general chemistry, J. Chem. Educ., 91 (2014) 1966–1970.

[212] V.K.K. Upadhyayula, V. Gadhamshetty, Appreciating the role of carbon nanotube composites in preventing biofouling and promoting biofilms on material surfaces in environmental engineering: a review, Biotechnol. Adv., 28 (2010) 802–816.

[213] M.R. Nabid, R. Sedghi, M. Behbahani, B. Arvan, M.M. Heravi, H.A. Oskooie, Application of poly 1,8-diaminonaphthalene/

multiwalled carbon nanotubes-COOH hybrid material as an efficient sorbent for trace determination of cadmium and lead ions in water samples, J. Mol. Recognit., 27 (2014) 421–428.

[214] W. Konicki, I. Pelech, E. Mijowska, I. Jasinska, Adsorption of anionic dye Direct Red 23 onto magnetic multi-walled carbon nanotubes-Fe$_3$C nanocomposite: kinetics, equilibrium and thermodynamics, Chem. Eng. J., 210 (2012) 87–95.

[215] T.S. Mthombo, A.K. Mishra, S.B. Mishra, B.B. Mamba, The adsorption behavior of Cu(II), Pb(II), and Co(II) of ethylene vinyl acetate-clinoptilolite nanocomposites, J. Appl. Polym. Sci., 121 (2011) 3414–3424.

[216] M. Khatamian, Z. Alaji, Efficient adsorption-photodegradation of 4-nitrophenol in aqueous solution by using ZnO/HZSM-5 nanocomposites, Desalination, 286 (2012) 248–253.

[217] M.N. Chong, Z.Y. Tneu, P.E. Poh, B. Jin, R. Aryal, Synthesis, characterisation and application of TiO$_2$-zeolite nanocomposites for the advanced treatment of industrial dye wastewater, J. Taiwan Inst. Chem. Eng., 50 (2015) 288–296.

[218] X.F. Tan, Y.G. Liu, Y.L. Gu, Y. Xu, G.M. Zeng, X.J. Hu, S.B. Liu, X. Wang, S.M. Liu, J. Li, Biochar-based nanocomposites for the decontamination of wastewater: a review, Bioresour. Technol., 212 (2016) 318–333.

[219] M. Zhang, B. Gao, S. Varnoosfaderani, A. Hebard, Y. Yao, M. Inyang, Preparation and characterization of a novel magnetic biochar for arsenic removal, Bioresour. Technol., 130 (2013) 457–462.

[220] M. Inyang, B. Gao, A. Zimmerman, M. Zhang, H. Chen, Synthesis, characterization, and dye sorption ability of carbon nanotube-biochar nanocomposites, Chem. Eng. J., 236 (2014) 39–46.

[221] M. Zhang, B. Gao, Y. Yao, Y.W. Xue, M. Inyang, Synthesis of porous MgO-biochar nanocomposites for removal of phosphate and nitrate from aqueous solutions, Chem. Eng. J., 210 (2012) 26–32.

[222] E.I. Unuabonah, A. Taubert, Clay-polymer nanocomposites (CPNs): adsorbents of the future for water treatment, Appl. Clay Sci., 99 (2014) 83–92.

[223] J.E. Bruna, A. Penaloza, A. Guarda, F. Rodriguez, M.J. Galotto, Development of MtCu(2+)/LDPE nanocomposites with antimicrobial activity for potential use in food packaging, Appl. Clay Sci., 58 (2012) 79–87.

[224] Y.S. Ho, J.C.Y. Ng, G. McKay, Kinetics of pollutant sorption by biosorbents: review, Sep. Purif. Rev., 29 (2000) 189–232.

[225] W. Plazinski, A. Plazinska, Equilibrium and Kinetic Modeling of Adsorption at Solid/Solution Interfaces, In: A. Bhatnagar, Ed., Application of Adsorbents for Water Pollution Control, Bentham Science Publishers, 2012, pp. 32–80.

[226] C. Gerente, V.K.C. Lee, P. Le Cloirec, G. Mckay, Application of chitosan for the removal of metals from wastewaters by adsorption-mechanisms and models review, Crit. Rev. Env. Sci. Technol., 37 (2007) 41–127.

[227] G.K. Sarma, S. Sen Gupta, K.G. Bhattacharyya, Adsorption of monoazo dyes (Crocein Orange G and Procion Red MX5B) from water using raw and acid-treated montmorillonite K10: insight into kinetics, isotherm, and thermodynamic parameters, Water Air Soil Pollut., 229 (2018) 312.

[228] A.M. Donia, A.A. Atia, F.I. Abouzayed, Preparation and characterization of nano-magnetic cellulose with fast kinetic properties towards the adsorption of some metal ions, Chem. Eng. J., 191 (2012) 22–30.

[229] X. Zhou, H. Yi, X. Tang, H. Deng, H. Liu, Thermodynamics for the adsorption of SO$_2$, NO and CO$_2$ from flue gas on activated carbon fiber, Chem. Eng. J., 200–202 (2012) 399–404.

[230] S. Mandal, M.K. Sahu, R. Kishore, Adsorption studies of arsenic (III) removal from water by zirconium polyacrylamide hybrid, Water Resour. Ind., 4 (2013) 51–67.

[231] V. Sureshkumar, S.C.G.K. Danie, K. Ruckmani, M. Sivakumar, Fabrication of chitosan—magnetite nanocomposite strip for chromium removal, Appl. Nanosci., 6 (2016) 277–285.

[232] H. Jabeen, K.C. Kemp, V. Chandra, Synthesis of nano zerovalent iron nanoparticles-graphene composite for the treatment of lead contaminated water, Journal of Environ. Manage., 130 (2013) 429–435.

[233] S.X. Dong, X.M. Dou, D. Mohan, C.U. Pittman Jr., J.M. Luo, Synthesis of graphene oxide/schwertmannite nanocomposites and their application in Sb(V) adsorption from water, Chem. Eng. J., 270 (2015) 205–214.

[234] F. Fang, L.T. Kong, J.R. Huang, S.B. Wu, K.S. Zhang, X.L. Wang, B. Sun, Z. Jin, J. Wang, X.J. Huang, J.H. Liu, Removal of cobalt ions from aqueous solution by an amination graphene oxide nanocomposite, J. Hazard. Mater., 270 (2014) 1–10.

[235] M. Machida, T. Mochimaru, H. Tatsumoto, Lead(II) adsorption onto the graphene layer of carbonaceous materials in aqueous solution, Carbon, 44 (2006) 2681–2688.

[236] Y.B. Sun, D.D. Shao, C.L. Chen, S.B. Yang, X.K. Wang, Highly efficient enrichment of radionuclides on graphene oxide-supported polyaniline, Environ. Sci. Technol., 47 (2013) 9904–9910.

[237] T. Yao, Y.P. Xiao, X.W. Wu, C.Y. Guo, Y.L. Zhao, X. Chen, Adsorption of Eu(III) on sulfonated graphene oxide: combined macroscopic and modeling techniques, J. Mol. Liq., 215 (2016) 443–448.

[238] R.M. Ashour, A.F. Abdel-Magied, A.A. Abdel-khalek, O.S. Helaly, M.M. Ali, Preparation and characterization of magnetic iron oxide nanoparticles functionalized by L-cysteine: adsorption and desorption behavior for rare earth metal ions, J. Environ. Chem. Eng., 4 (2016) 3114–3121.

[239] Y. Tan, M. Chen, Y. Hao, High efficient removal of Pb (II) by amino-functionalized Fe3O4 magnetic nano particles, Chem. Eng. J., 191 (2012) 104–111.

[240] A.S. Poursani, A. Nilchi, A.H. Hassani, M. Shariat, J. Nouri, A novel method for synthesis of nano-γ-Al$_2$O$_3$: study of adsorption behavior of chromium, nickel, cadmium and lead ions, Int. J. Environ. Sci. Technol., 12 (2015) 2003–2014.

[241] J.S. Azizian, M. Bagheri, Enhanced adsorption of Cu^{2+} from aqueous solution by Ag doped nano-structured ZnO, J. Mol. Liq., 196 (2014) 198–203.

[242] I. Mobasherpour, E. Salahi, M. Ebrahimi, Removal of divalent nickel cations from aqueous solution by multi-walled carbon nanotubes: equilibrium and kinetic processes, Res. Chem. Intermed., 38 (2012) 2205–2222.

[243] Y. Ren, N. Yan, Q. Wen, Z. Fan, T. Wei, M. Zhang, J. Ma, Graphene/δ-MnO$_2$ composite as adsorbent for the removal of nickel ions from wastewater, Chem. Eng. J., 175 (2011) 1–7.

[244] L. Yang, Z. Li, G. Nie, Z. Zhang, X. Lu, C. Wang, Fabrication of poly(o-phenylenediamine)/reduced graphene oxide composite nanosheets via microwave heating and their effective adsorption of lead ions, Appl. Surf. Sci., 307 (2014) 601–607.

[245] A. Sharma, B. Lee, Cd (II) removal and recovery enhancement by using acrylamide—titanium anocomposite as an adsorbent, Appl. Surf. Sci., 313 (2014) 624–632.

[246] W. Jung, B.H. Jeon, D.W. Cho, H.S. Roh, Y. Cho, S.J. Kim, D.S. Lee, Sorptive removal of heavy metals with nano-sized carbon immobilized alginate beads, J. Ind. Eng. Chem., 26 (2015) 364–369.

[247] K. Xie, L. Jing, W. Zhao, Y. Zhang, Adsorption removal of Cu^{2+} and Ni^{2+} from waste water using nano-cellulose hybrids containing reactive polyhedral oligomeric silsesquioxanes, J. Appl. Polym. Sci., 22 (2011) 2864–2868.

[248] S.B. Khan, K.A. Alamry, H.M. Marwani, A.M. Asiri, M.M. Rahman, Synthesis and environmental applications of cellulose/ZrO$_2$ nanohybrid as a selective adsorbent for nickel ion, Composites Part B, 50 (2013) 253–258.

[249] G.N. Kousalya, M.R. Gandhi, S. Meenakshi, Removal of toxic Cr (VI) ions from aqueous solution using nano-hydroxyapatite-based chitin and chitosan hybrid composites, Adsorpt. Sci. Technol., 28 (2010) 49–64.

[250] A.F. El-Kafrawy, S.M. El-Saeed, R.K. Farag, H. Al-Aidy El-Saied, M. El-Sayed Abdel-Raouf, Adsorbents based on natural polymers for removal of some heavy metals from aqueous solution, Egypt. J. Pet., 26 (2017) 23–32.

[251] L. Yang, X. Chu, F. Wang, Y. Li, L. Zhang, Investigation of selective and effective recovery of noble metal osmium by adsorption onto nano Al$_2$O$_3$ particles, New J. Chem., 38 (2014) 3250–3257.